AD-A115 633 NORTHWESTERN UNIV EVANSTON IL DEPT OF MATERIALS SCIENCE F/G 20/11
RESIDUAL STRESSES AND SLIDING WEAR.(U)
MAY 82 J W HO, C NOYAN, J B COHEN, V D KHANNA N00014-80-C-0116
UNCLASSIFIED TR-7 NL

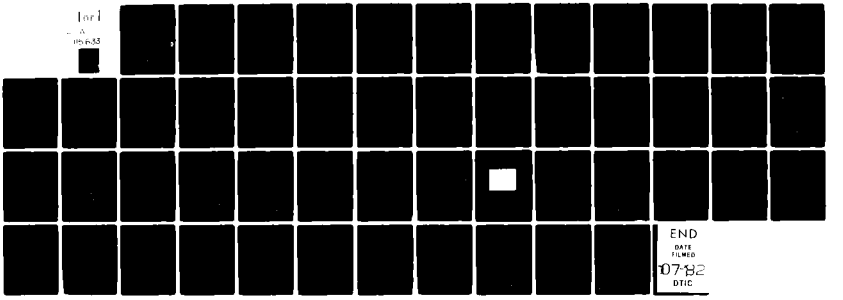

END
DATE FILMED
07-82
DTIC

NORTHWESTERN UNIVERSITY

DEPARTMENT OF MATERIALS SCIENCE

Technical Report No. 7
May 25, 1982

Office of Naval Research
Contract Nooo14-80-C-0116

RESIDUAL STRESSES AND SLIDING WEAR

BY

J. W. Ho, C. Noyan, J. B. Cohen, V. D. Khanna and Z. Eliezer

EVANSTON, ILLINOIS

RESIDUAL STRESSES AND SLIDING WEAR

ABSTRACT

The residual stresses that develop during wear of SAE 1018 and 4340 steel have been examined. The entire three-dimensional stress tensor was obtained. A normal stress perpendicular to the surface, predicted by theory, has been found, but its magnitude is too small to affect the wear rate. There are also significant shear stresses. The wear process rapidly alters any initial stress distribution produced by heat treatment or peening to such a degree that the wear rate is not affected by these stresses, unless they are initially larger than those that can be produced by the wear parameters.

Residual Stresses and Sliding Wear

J.W. Ho*, C. Noyan and J.B. Cohen
Department of Materials Science and Engineering
The Technological Institute
Northwestern University
Evanston, Illinois 60201

V.D. Khanna and Z. Eliezer
Department of Mechanical Engineering and
Materials Science and Engineering Program
The University of Texas at Austin
Austin, Texas 78712

I. INTRODUCTION

In recent years, a new theory for sliding wear has been proposed by Suh and his co-workers [1]. According to this theory, cracks initiate beneath the surface and propagate parallel to the surface in a wearing material. The spread of such cracks results in the formation of lamellae which eventually separate. The cyclic loading occurring during wear contributes to crack propagation in a way similar to that in fatigue. It is well known that residual stress strongly influences fatigue behavior [2] and consequently, changes in residual stress during sliding might be expected to influence wear behavior.

The purpose of this paper is:

a) to determine the nature (sign and magnitude) of residual stresses induced by sliding motion, and:

b) to determine the influence of pre-existing residual stresses on the wear behavior of steels.

---

*Currently at the Research Institute on Strength of Materials, Xian Jiaotong University, Xian, Shaanxi, The People's Republic of China.

Residual stresses produced in rolling contacts have been calculated by Merwin and Johnson [3]. They assumed that when a solid is under load, a compression normal to the surface is produced. However the decrease in this dimension cannot occur without resistance from the part. Therefore, compressive residual stresses develop in a plane parallel to the surface to prevent further yielding. The model is simplified since both plane-stress and no strain hardening are assumed. Thus, no residual stress perpendicular to the surface is considered, and all shear components are nil.

Suh and coworkers have employed Merwin and Johnson's model to calculate the residual stress distribution after sliding wear by considering a tangential force acting in the surface. The results of their calculations are shown in Fig. 1a [4]. It can be seen that the higher the friction coefficient the larger the compressive stress σ_{11} (in a plane parallel to the surface and in the direction of sliding) and the closer is its maximum to the surface. They pointed out that these residual stresses probably contribute to sub-surface crack initiation in two-phase materials. However, these stresses would not influence crack propagation in a plane parallel to the surface. Therefore, when crack propagation is much slower than crack initiation, residual stresses should have little effect on wear rate.

Recently, Chiu [5] reconsidered the case of rolling contact, taking into account strain hardening during plastic deformation. His calculations (for SAE 52100 at a hardness level of 58.5 R_c under

a pressure of 3.85 GPa) are shown in Fig. 1b. A tensile stress perpendicular to the surface (σ_{33}) exists at a certain depth from the surface. Chiu suggested that this residual tensile stress might contribute to crack initiation. However, while the yield strength of SAE 52100 (at R_c 58.5) is ~3000 MPa [5], the calculated value of the maximum residual stress is only ~20 MPa. This value seems to be too small to affect crack initiation. Actually, experiments done using parameters similar to those used by Chiu in his calculations showed [6] that σ_{11} and σ_{22} can reach ~800-1000 MPa. If σ_{33} was comparable to these values, it would indeed effect the wear rate. It is evident that an experimental determination of σ_{33} would be of considerable interest.

The effect of σ_{11} and σ_{22} on wear rate is still unclear. Some authors [7,8] conclude that the larger the compressive residual stresses (σ_{11} and/or σ_{22}) the lower the wear rate. Unfortunately, these authors did not separate the effect of hardness from that of residual stresses. When the residual stresses are altered by either plastic deformation or heat treatment, the hardness also changes. Since the wear rate is hardness dependent, changes in the residual stresses can be expected to be correlated with changes in wear rate under such circumstances.

In order to eliminate hardness as a variable, investigators have employed a loading stress to simulate residual stress, for example reference [9]. Their results showed that the larger the tensile loading stress on the sample the higher the wear rate.

However, residual stresses may change during wear, so the actual effect may be different than that resulting from a constant loading stress.

II. DETERMINATION OF THE STRESS TENSOR: THEORETICAL CONSIDERATIONS

The stresses in surface layers can be measured by x-ray diffraction methods [10], since they alter the shape of the interplanar spacing (d_ψ) vs $\sin^2\psi$ (Fig. 2), where ψ is the angle between the normal to the surface and the normal to the diffracting planes.

The main equations for x-ray measurements of stress have recently been generalized to include the stress normal to the surface [11]. With subscript 3 indicating this direction, the strain ε'_{33} can be written as:

$$\varepsilon'_{33} = \frac{d_{\phi\psi}-d_o}{d_o} = \langle\varepsilon_{11}\rangle\cos^2\phi\sin^2\psi$$

$$+ \langle\varepsilon_{12}\rangle\sin2\phi\sin^2\psi + \langle\varepsilon_{13}\rangle\cos\phi\sin2\psi + \langle\varepsilon_{22}\rangle\sin^2\phi\sin^2\psi$$

$$+ \langle\varepsilon_{23}\rangle\sin\phi\sin2\psi + \langle\varepsilon_{33}\rangle\cos^2\psi \qquad (1)$$

$$\langle\sigma_{ij}\rangle = \frac{1}{\frac{1}{2}S_2(hk\ell)}\left[\langle\varepsilon_{ij}\rangle - \delta_{ij}\frac{S_1(hk\ell)}{\frac{1}{2}S_2(hk\ell)+3S_1(hk\ell)}\Sigma\varepsilon_{ii}\right] \qquad (2)$$

The $\langle\sigma_{ij}\rangle$ and $\langle\varepsilon_{ij}\rangle$ are average values of stress and strain in the volume associated with the x-ray penetration depth, S_1 and S_2 are elastic constants for the $(hk\ell)$ planes. d_o is the stress-free

d-spacing of the (hkℓ) planes, and ϕ is the angle on the surface from the principal stress axis (Fig. 2).

Now let:

$$a_1 \equiv \tfrac{1}{2}[\langle\varepsilon_{\phi\Psi+}\rangle + \langle\varepsilon_{\phi\Psi-}\rangle]$$

$$= \frac{\langle d_{\phi\Psi+}\rangle + \langle d_{\phi\Psi-}\rangle}{2d_o} - 1$$

$$= \langle\varepsilon_{33}\rangle + [\langle\varepsilon_{11}\rangle\cos^2\phi + \langle\varepsilon_{12}\rangle\sin 2\phi + \langle\varepsilon_{22}\rangle\sin^2\phi - \langle\varepsilon_{33}\rangle]\sin^2\Psi, \quad (3)$$

and:

$$a_2 \equiv \tfrac{1}{2}[\langle\varepsilon_{\phi\Psi+}\rangle - \langle\varepsilon_{\phi\Psi-}\rangle] = \frac{\langle d_{\phi\Psi+}\rangle - \langle d_{\phi\Psi-}\rangle}{2d_o}$$

$$= [\langle\varepsilon_{13}\rangle\cos\phi + \langle\varepsilon_{23}\rangle\sin\phi]\sin|2\Psi| \quad (4)$$

Measuring $d_{\phi\Psi+}$ and $d_{\phi\Psi-}$ at $+\Psi$ and $-\Psi$ tilts, a_1 and a_2 can be determined. The value of $\langle\varepsilon_{33}\rangle$ is obtained from the intercept of a_1 vs $\sin^2\Psi$ if d_o is known. The tensor components $\langle\varepsilon_{11}\rangle$, $\langle\varepsilon_{12}\rangle$ and $\langle\varepsilon_{22}\rangle$ are obtained from $\partial a_1/\partial\sin^2\Psi$. For ϕ=90°, $[\langle\varepsilon_{22}\rangle - \langle\varepsilon_{33}\rangle]$ is evaluated. The tensor component $\langle\varepsilon_{12}\rangle$ can be obtained from $\partial a_1/\partial\sin^2\Psi$ at φ=45°. From $\partial a_2/\partial\sin|2\Psi|$, $\langle\varepsilon_{13}\rangle$ results when ϕ=0, and $\langle\varepsilon_{23}\rangle$ when ϕ=90°.

With this x-ray diffraction method, the residual stress tensor can be measured vs depth below the surface by etching. These stresses will reach a new balance after each etch. If only a small window is so etched, and the removed layer is very thin

compared to the cross section of the sample, it will not appreciably perturb the initial distribution of σ_{11} and σ_{22}. However, it will affect the distribution of σ_{33}, since this component is always zero at the surface. The measured value is an average over a certain depth. Once a layer has been etched away, σ_{33} again falls to zero at the exposed surface, regardless of its initial value at this depth before etching. One possible way to circumvent this problem is by using several x-ray wavelengths to obtain several average σ_{33} values with different penetration depths, and then to interpolate. More work has to be done to test this possibility in practice. For our purposes, to avoid this correction, we chose the wear test parameters so as to produce delamination within the x-ray penetration depth. Experiments reveal that cracks may propagate parallel to the surface at depths of ≈ 5 μ [12]. This is just the penetration depth for Cr radiation in steel. The wear parameters were selected to be similar to those in reference [12], and the depth at which cracks formed was determined by SEM. We will focus on the measurement of σ_{33} in the first layer; other values are given only to suggest the variation with depth.

III. EXPERIMENTAL PROCEDURES

A. Sample Preparation

Two groups of specimens were prepared, from SAE 1018 and 4340 steel. The mechanical and thermal treatments are shown in Table 1. SAE 1018 discs of 75 mm diameter were cut from 300x300x6 mm plates.

After austenitizing at 980°C and quenching into ice brine, they were tempered* at 680°C for 2 hours. The surface was ground (under coolant) to remove the decarburized layer and polished through 600 grit emery paper. Back reflection Debye-Scherrer rings were examined with unfiltered Co radiation after etching off the surface layer. These rings were uniform, indicating that the grain size was fine and that there was no appreciable preferred orientation.

Referring to Table 1, the sample labeled A was obtained by annealing at 420-440°C for 1 hour under a pressure of $3\text{-}4\times10^{-6}$ torr. Specimen AS was obtained by shot peening, to induce compressive stresses. However, the shot peening process also led to an increase in hardness. In order to separate these two factors (residual stress and hardness), a sample was prepared in the following way. An annealed disc was bent into a dome (of depth 2-4 mm), shot peened on the concave side, then flattened to release the residual stress by plastic deformation. This sample was labeled AF. Since the shot peening intensity was the same for the AS and AF samples the resulting hardness was the same, while the residual stress pattern was different.

The SAE 4340 discs (4 mm thick) were cut from a 50 mm diameter rod. After quenching in oil from 840°C, they were tempered (at 420-430°C) for 1.5 hours to a hardness of R_c 44. Again, three sets of specimens were prepared (Table 1): hardened (H), hardened and shot peened (HS), hardened, bent, shot peened and flattened (HF). Finally all specimens were polished through 600 grit emery paper.

*all tempering was done in air

The tempering temperature of the hardened sample was selected so as to eliminate residual stresses induced during quenching and yet retain a high yield strength. The reported ultimate tensile strength of 4340 steel for tempering at 425°C is ≈1,500 MPa, while the yield strength is ≈1,400 MPa [13]. Due to this small difference between the UTS and yield values, plastic deformation is limited. The hardness of the shot peened sample is similar to that after tempering, while the residual stress distribution is quite different.

5) Wear Tests

Sliding wear was carried out on a pin-on-disc type machine [14]. All experiments were performed in air, at ambient pressure and temperature. The cylindrical pin was made of a hardened SAE O1 tool steel, and had a diameter of 6.35 mm. The friction force was measured with a strain ring while the wear of the disc was obtained with a linear variable displacement transducer (LVDT). The pin displacements were read from the recorder chart and plotted as a function of time. From such plots, via a least square regression procedure, the steady state wear rate of the disc was determined.

For the hardened discs, the wear rates were calculated from the LVDT measurements, and, as well, from weight loss. The experimental parameters employed in all wear tests are given in Table 2.

C) Measurements of Residual Stress by X-Rays

A Picker diffractometer equipped with a quarter-circle goniometer, a scintillation detector and pulse height analyzer were employed. The divergence slit and receiving slit were 1° and 0.4°, respectively. The irradiated spot on a specimen was limited (with lead at the divergence slit) to 2x2 mm to keep the x-ray beam on the worn track, even at high Ψ tilt angles. Cr radiation was employed to examine the (211) peak. For each of the ϕ angles of 0, 45 and 90°, eleven Ψ-tilts were chosen: 0, ±18.43, ±26.57, ±33.21, ±39.23, and ±45 degrees. The ϕ tilts were made about an axis parallel to the plane of diffraction; Ψ was about an axis normal to this plane. Altogether, 33 peaks were examined to solve eq. 1 by least squares for the six strain components. All the experimental data were accumulated and analyzed with the aid of a DEC PDP 8/E mini-computer.

The elastic constants employed in the data analysis were calculated from single crystal compliances according to Kröner's theory of bulk elasticity, which assumes an anisotropic crystal coupled to isotropic surroundings [15, 16].

$$S_1\ (211) = -0.125 \times 10^{-5}\ \text{MPa}$$

$$\tfrac{1}{2}S_2\ (211) = 0.577 \times 10^{-5}\ \text{MPa}$$

Special consideration was given to the following:

1) K_α-doublet correction.

Because a stationary receiving slit was employed, the K_{α_1}-K_{α_2} doublet resolution varied from the annealed to the shot peened specimens, and with the various Ψ-tilts. The apparent peak position of the K_{α_1} radiation is influenced to some extent by the K_{α_2} component, depending on the width of the profile. For Cr-K_α and the (211) peak a correction was applied if the half-width was broader than ~1.4° [17].

ii) Angular dependent intensity corrections.

Intensities were corrected for the Lorenz-polarization and absorption factors, and also for the background (which was measured at 151° 2θ for the annealed samples, and 150° 2θ for the hardened samples). After correction, the peak position was determined by a five-point parabolic fit to the top 15 percent of the peak.

iii) Sample alignment.

Peak positions obtained with the stationary slit method, (employed in this work) are not very sensitive to sample displacement. Nevertheless, absolute values of d-spacing ($d_{\phi\Psi}$) are required in eq. 1 for the stress tensor calculation. The sample displacement can be obtained from the slope of the lattice parameter vs. Nelson-Riley factor [18]. A linear least-square fit for the (110), (220) and (211) peaks was employed. The displacement was then adjusted to within 25 μm of the center of the goniometer. (The Lorenz-polarization, absorption, and doublet corrections were included in the alignment procedure.)

The ambient temperature was kept constant to within 2-3°C.

iv) Stress-free lattice parameter, a_o .

The d_o value is important for the calculations of the normal components of the stress tensor. In these experiments, for instance, if a_o increased by 0.0001 Å, the tensile normal stresses would decrease by ~17 MPa, and the compressive normal stress would increase by an equal amount.

Tempering at 420-430°C is sufficient to release the macro-residual stresses of a quenched sample. The a_o values of both steels were examined on a spot which was exposed by etching to a depth ~100 μm from the surface. First, the fresh surface was examined. If the stress was within ±10 MPa, the sample was realigned to reduce the displacement to 10 μm. Then measurements were made at all 33 values of ϕ,Ψ. The value of a_o was determined from the average of these 33 peak positions:

annealed 1018 sample - 2.86640(5) Å

hardened and tempered 4340 sample - 2.86760(9) Å

The values in parentheses represent the errors.

v) Effects of stress gradient.

The effects of the stress gradient and layer removal were estimated. The first altered the stresses 10 percent or less. The latter caused a change of only ~2 percent, with the assumption that an entire layer was removed. As only a window was removed, the effect is even smaller.

D) Hardness Tests

The Vickers hardness of annealed 1018 samples was determined from an average of six readings taken with a load of 50 g. For the hardened 4340 samples, the average of at least twelve readings was employed, with a 100 g load. The hardness variation vs depth was determined by etching with the same solution as used in the measurements of the stress distribution, namely 200 parts 30% H_2O_2 and 15 parts 48% HF, contained in an ice-water bath.

IV. RESULTS AND DISCUSSION

A) Annealed Samples (SAE 1018)

Before wear, the annealed samples contained fairly low residual stresses (Fig. 3) which probably were induced by cooling after the vacuum anneal. The AS sample (annealed and shot peened) displays compressive stresses σ_{11} and σ_{22} of equal magnitude (Fig. 3b). The distribution vs. depth is typical after shot peening.

Sample AF (annealed, bent, shot peened, and flattened) exhibits a quite different distribution than that for AS, for both σ_{11} and σ_{22} (Fig. 3c). The value of σ_{11} is zero at a depth of ≈ 25 μm. The large compressive value for σ_{11} at the surface is due to polishing (performed in order to obtain the same initial roughness for all samples). The value of σ_{22}, which is probably less important than σ_{11} for wear resistance, remains compressive for large depths but its value is smaller than in sample AS. The stress component σ_{33}, and the shear components, are nearly zero in these three samples.

Before wear, the hardness distributions in the AS and AF samples are similar, but different from that in sample A (Fig. 4). After wear, cracks were found in a drastically deformed layer within ~10 μm beneath the surface (Fig. 5). The value of σ_{23} in this layer is tensile (in agreement with expectations), but its magnitude is only ~40 MPa, much smaller than that of σ_{11} or σ_{22} (Fig. 6).

Comparing Figs. 3a and 6a, it can be seen that σ_{11} and σ_{22} change their distribution with wear, but only over a depth of ~75 μm. Within this depth the distributions of σ_{11} and σ_{22} in the worn track are similar for all worn samples, and so are the hardness distributions (Fig. 4).

The wear rates were calculated at steady state. Usually, this required a couple of hours. In order to discover how soon the final residual stress pattern develops, measurements were made on a worn track after only 100 revolutions. The similarity between Fig. 7 and Fig. 6a shows that the final pattern is established in only a few minutes of wear.

Shear stresses in the worn track are not significant, except for σ_{13}. Fig. 8 shows that σ_{13} has a maximum value of ~-35 MPa at the surface and decreases through the depth. The negative sign indicates that the shear residual stress is opposite to the direction of motion of the pin.

In order to compare the magnitude of the residual and loading stresses, the contact stress between two flat surfaces has been

evaluated following Greenwood [19]. When parabolic asperities with a height distribution close to Gaussian are brought into contact with a flat surface in the absence of any tangential force, the total number of contacts N(d) can be expressed as:

$$N(d) = 4\pi\,(\eta\beta\sigma)\eta\;A.F(\frac{d}{\sigma}) \qquad (5)$$

where η, β and σ are density, tip radius of curvature and standard deviation (of peak height) of the asperities, respectively. Here, $\eta\cdot\beta\cdot\sigma$ is an empirical number known to be about 0.05, A is the apparent area of contact, d is the apparent distance between asperities and $F(\frac{d}{\sigma})$ depends on the nominal pressure and takes on a value of 0.027 [19] at a pressure of 3.15 kgf/cm^2. If η and σ are assumed to be 2000/mm^2 and 5×10^{-5}mm, respectively, N(d) is 1150.

By distributing the loading force over the number of contacts N(d), the Hertzian stress was estimated. Its value, σ_{max}, was ~1300 MPa at a depth of ~1.8 μm. If the tangential stress were taken into account the shear stress could be as large as 0.4 σ_{max} within 1 μm, and for a friction coefficient larger than 0.4.

The fact that the residual stresses tend to be identical in the worn surfaces independent of their initial distribution and that their magnitude is much lower than that of the loading stress explains why the wear rates of all the annealed samples are similar (Table 3).

c) Hardened Samples (SAE 4340)

Before wear, the residual stress distributions in samples H and HS were different (Fig. 9a,b). The bending process did not significantly change σ_{11} or σ_{33} (Fig. 9c); plastic deformation was limited in this spring leaf-like sample.

The hardness values were essentially the same for all three hardened samples before and after wear, and through the depth (Fig. 10). The distribution of residual stresses after wear (Fig. 11) shows that the depth influenced by wear was only ~25 μ, much less than that in the annealed samples. The value of σ_{33} was ~50 MPa on the surface, while the shear stresses (Fig. 12) were in the range of ~125 to ~175 MPa. The wear rates and the friction coefficients of the hardened samples are higher than those after shot peening (Table 4). As their hardness is the same (Fig. 10a), this difference probably results from the different initial stress distribution in these samples. In the hardened sample (H) the wear process changes the initial stress distribution, inducing large compressive σ_{11} and σ_{22} components near the surface. In sample HS, on the other hand, the stress distribution after wear is hardly distinguishable from the initial one; perhaps, the large initial σ_{11} and σ_{22} prevent deformation in the surface layer, thus resulting in a low wear rate.

In a study on the relationship between delamination wear and fatigue cracks, Ritchie [20] suggested that wear rates correlate with microcracks, not with macrocracks. It is possible

that the hardened two phase material is somewhat more homogeneous after shot peening, thus keeping microcracks from propagating; in such a case, a lower wear rate would also result.

By and large the friction coefficient depends on the same type of parameters as the wear rate [21]. Accordingly, the difference between the friction coefficients of the H and HS samples can be explained along the same lines.

V. CONCLUSIONS

1. Although a residual stress component normal to the surface (σ_{33}) does exist in a worn surface, its magnitude is much lower than that for σ_{11} and σ_{22}. It is unlikely that it would affect the wear rate to a significant extent.

2. The only shear stress which is appreciable in a worn surface is σ_{13}. Its maximum values are ~35 MPa and 125-175 MPa for annealed and hardened samples, respectively. Its direction is opposite to the pin motion direction. As such, it may contribute to crack propagation.

3. Residual stresses build up in the early stages of wear and any initial stress pattern is destroyed. This is true for both the annealed and the hardened steel, with the exception of the hardened and shot-peened sample. In this latter specimen the initial σ_{11} and σ_{22} were larger than could eventually be induced by the sliding action under our experimental conditions.

4. Because the sliding action changes residual stresses to a common pattern, the wear rate is virtually independent of the initial stress distribution, unless the initial stress pattern involves values larger than those produced by wear.

ACKNOWLEDGEMENTS

This research was supported at Northwestern University by ONR, and at The University of Texas by the Houston Lighting and Power Company. The joint effort was initiated while one of the authors (JBC) was a visiting professor at The University of Texas. Sample preparation, x-ray measurements and hardness were carried out at Northwestern University, the former in the x-ray diffraction facility of Northwestern's Materials Research Center, supported in part by NSF grant no. DMR-76-80847. The authors would like to thank Metal Improvement Company for carrying out the shot peening.

References

1. N.P. Suh, "An Overview of the Delamination Theory of Wear, Wear, Netherland 44 (1977) 1-16.

2. Alman and Black, Residual Stresses and Fatigue In Metals, McGraw Hill Book Co. (1964).

3. J.E. Merwin and K.L. Johnson, "An Analysis of Plastic Deformation in Rolling Contact," Proc. Inst. Mech. Eng., London, 177 (1963) 676-690.

4. S. Jahanmir and N.P. Suh, "Mechanics of Subsurface Void Nucleation in Delamination Wear," Wear, Netherland 44 (1977) 17-38.

5. Y.P. Chiu, "On the Plastic Growth and Residual Stresses Due to Contact Load Applied in Two Stages," Solid Contact and Lubrication, AMD 39 (1980) 193-204.

6. H. Muro, N. Tsushima and K. Nundme, "Failure Analysis of Rolling Bearings by X-Ray Measurement of Residual Stress," Wear, Netherland 25 (1973) 345-356.

7. Toshimi Sasaki, et al. "A Study on the Stress Induced in the Sliding Surface of Hardened 0.4%C Steels under a Dry Condition Journal of Japanese Metal Society 38 (1974) 599-603.

8. Toshihiro Yamada, et al. "A Study on Wear Characteristics and the Stress Induced in the Sliding Surface of Hardened Steel Under Dry Condition," Journal of Japanese Metal Society 39 (1975) 1199-1204.

9. Kichiro Endo, et al. "Influence of Internal Stresses on the Wear of Steel," Japan Precision Machine 37 (1971) 496-501.

10. B.D. Cullity, Elements of X-Ray Diffraction, Addison-Wesley (1978) 447-479.

11. H. Dölle, "Influence of Multiaxial Stress States, Stress Gradients and Elastic Anisotropy on the Evaluation of Stress by X-Rays, J. Appl. Cryst. 12 (1979) 489-501.

12. N. Saka, A.M. Eleiche, N.P. Suh, Wear of Metals at High Sliding Speeds, Wear, Netherland 44 (1977) 109-125.

13. Bammeister, Avallone, Mark's Standard Handbook for Material Engineers, (1978).

14. V.G. Khanna, "Effect of Thermoelectric Current on the Friction and Wear Behavior of an Iron-Constantan Couple," Masters Thesis, The University of Texas at Austin, 1977.

15. E. Kröner, "Elastic Moduli of Perfectly Disordered Composite Materials," J. Mech. Phys. Solid 15 (1967) 319-329.

16. G. Simmons and H. Wang, Single Crystal Elastic Constants and Aggregate Properties, The MIT Press, Cambridge, MA, 1971.

17. J.B. Conen, H. Dölle and M.R. James, "Determining Stresses from X-ray Powder Patterns," in NBS Spec. Publ. 567, Feb. 1980, pp. 453-477 (Symposium on Accuracy in Powder Diffraction).

18. L.H. Schwartz and J.B. Cohen, Diffraction from Materials, Academic Press (1977) 245-246.

19. J.A. Greenwood and J.H. Tripp, "The Contact of Two Nominally Flat Rough Surfaces," Proc. Inst. Mech. Engrs. 185 (1971) 625-633.

20. R.O. Ritchie, "On the Relationship Between Delamination Wear and the Initiation and Growth of Fatigue Cracks in Ultrahigh Strength Steel," in Fundamentals of Tribology, MIT Press (1978) 127-134.

21. N. Saka, "Effect of Microstructure on Friction and Wear of Metals," in Fundamentals of Tribology, MIT Press (1978) 135-170.

Table 1

Mechanical and Thermal Treatments of Samples

Specimen Label	Steel	Treatment
A	1018	Vacuum Annealed and Polished
AW	1018	Vacuum Annealed, Polished and Worn
AS	1018	Annealed, Shot Peened and Polished
ASW	1018	Annealed, Shot Peened, Polished and Worn
AF	1018	Annealed, Bent, Shot Peened, Flattened and Polished
AFW	1018	Annealed, Bent, Shot Peened, Flattened, Polished and Worn
H	4340	Hardened and Polished
HW	4340	Hardened, Polished and Worn
HS	4340	Hardened, Shot Peened and Polished
HSW	4340	Hardened, Shot Peened, Polished and Worn
HF	4340	Hardened, Bent, Shot Peened, Flattened and Polished
HFW	4340	Hardened, Bent, Shot Peened, Flattened, Polished and Worn

Table 2

Parameters During Wear

Wear Parameter	Annealed Sample	Hardened Sample
Load N	9.62	22.3
Velocity, m/sec	0.15	0.069
Diameter of Track, mm	50	35

Table 3

Friction and Wear Values for SAE 1018 Samples

Parameter	Sample		
	A	AS	AF
Temperature, °C	23.3	23.3	23.3
Relative Humidity, %	64	64	64
Friction Coefficient	.566	.564	.572
Wear Rate, mm^3/km	.239	.285	.297

Table 4

Friction and Wear Values for SAE 4340 Samples

	H		HS	
Parameter	1	2	1	2
Temperature, °C	23.3	23.3	24.4	23.2
Relative Humidity, %	40	40	58	37
Friction Coefficient	.785	.813	.583	.68
Wear Rate, mm^3/km	.011	.012	.00284	.00117

Legend to Illustrations

Fig. 1. a) Residual stresses produced by sliding wear. p=loading stress; k=yield strength in shear; μ=friction coefficient; y=depth from the surface; a=half contact length of an asperity (from ref. [4]).

b) Residual stresses produced by rolling contact. y=depth from the surface; a=half contact length. σ_{33} and σ_{11} are the stresses perpendicular to the surface and parallel to the worn track, respectively (from ref. [5]).

Fig. 2. Geometry for x-ray diffraction measurement of stress. Interplanar spacing measured along L_3.

Fig. 3. Residual stresses in SAE 1018 steel, prior to wear.

a) Sample A (annealed).

b) Sample AS (annealed and shot peened).

c) Sample AF (annealed, bent, shot peened and flattened).

□: σ_{11}; O: σ_{22}; Δ: σ_{33}.

Fig. 4. Vickers Hardness of 1018 steel.

a) Samples A (Δ) and AW (+).

b) Samples AS (Δ) and ASW (+).

c) Samples AF (Δ) and AFW (+).

Fig. 5. Crack under worn track. Sample plated with electroless Ni prior to sectioning.

Fig. 6. Residual stresses in 1018 steel after wear.

a) Sample AW (sample A, after wear).

Fig. 6. b) Sample ASW (sample AS, after wear).

c) Sample AFW (sample AF, after wear).

□: σ_{11}; ○: σ_{22}; Δ: σ_{33}.

Fig. 7. Residual stresses under the worn track of sample A after 100 revolutions. □: σ_{11}; ○: σ_{22}; Δ: σ_{33}.

Fig. 8. Shear residual stress (σ_{13}) on sample A.

□: AW; ○: ASW; Δ: AFW; +: A100W.

Fig. 9 Residual stresses in SAE 4340 quenched and tempered to R_c 44.

a) Sample H

b) Sample HS (quenched, tempered to R_c 44, and shot peened)

c) Sample HF (quenched, tempered to R_c 44, bent, shot peened and flattened).

□: σ_{11}; ○: σ_{22}; Δ: σ_{33}.

Fig. 10. Vickers Hardness, 4340 steel.

a) Samples H (Δ), HW (+), HS (X) and HSW (□).

b) Samples HF (Δ) and HFW (+).

Fig. 11. Residual stresses in 4340 steel after wear.

a) Sample HW (sample H, after wear).

b) Sample HSW (sample HS, after wear).

c) Sample HFW (sample HF, after wear).

□: σ_{11}; ○: σ_{22}; Δ: σ_{33}.

Fig. 12. Shear stresses, σ_{13}, in worn 4340 steel.

□: HW; ○: HSW; Δ: HFW.

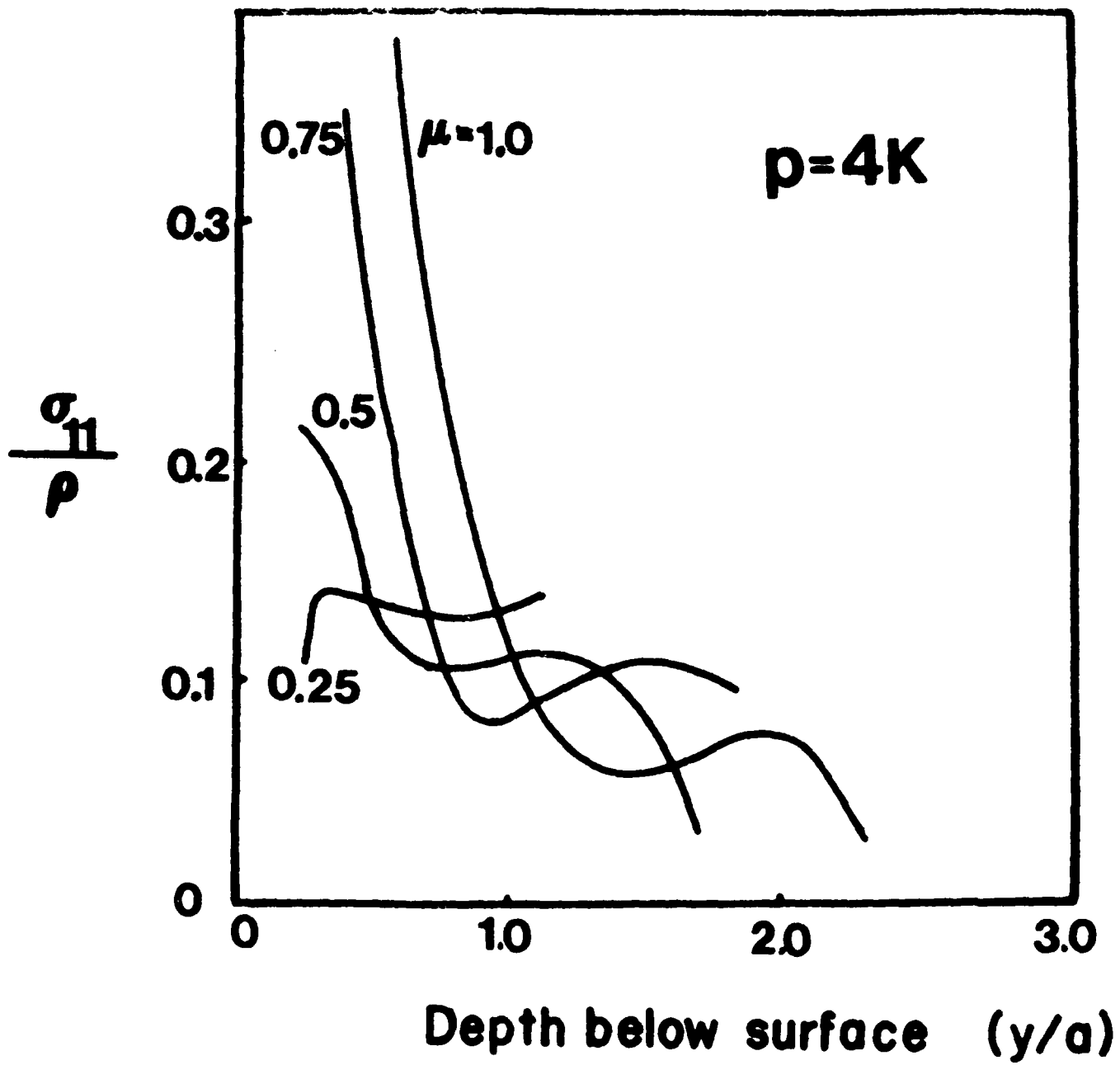

Ho, Noyan, Cohen, Khanna & Eliezer

FIGURE 1a

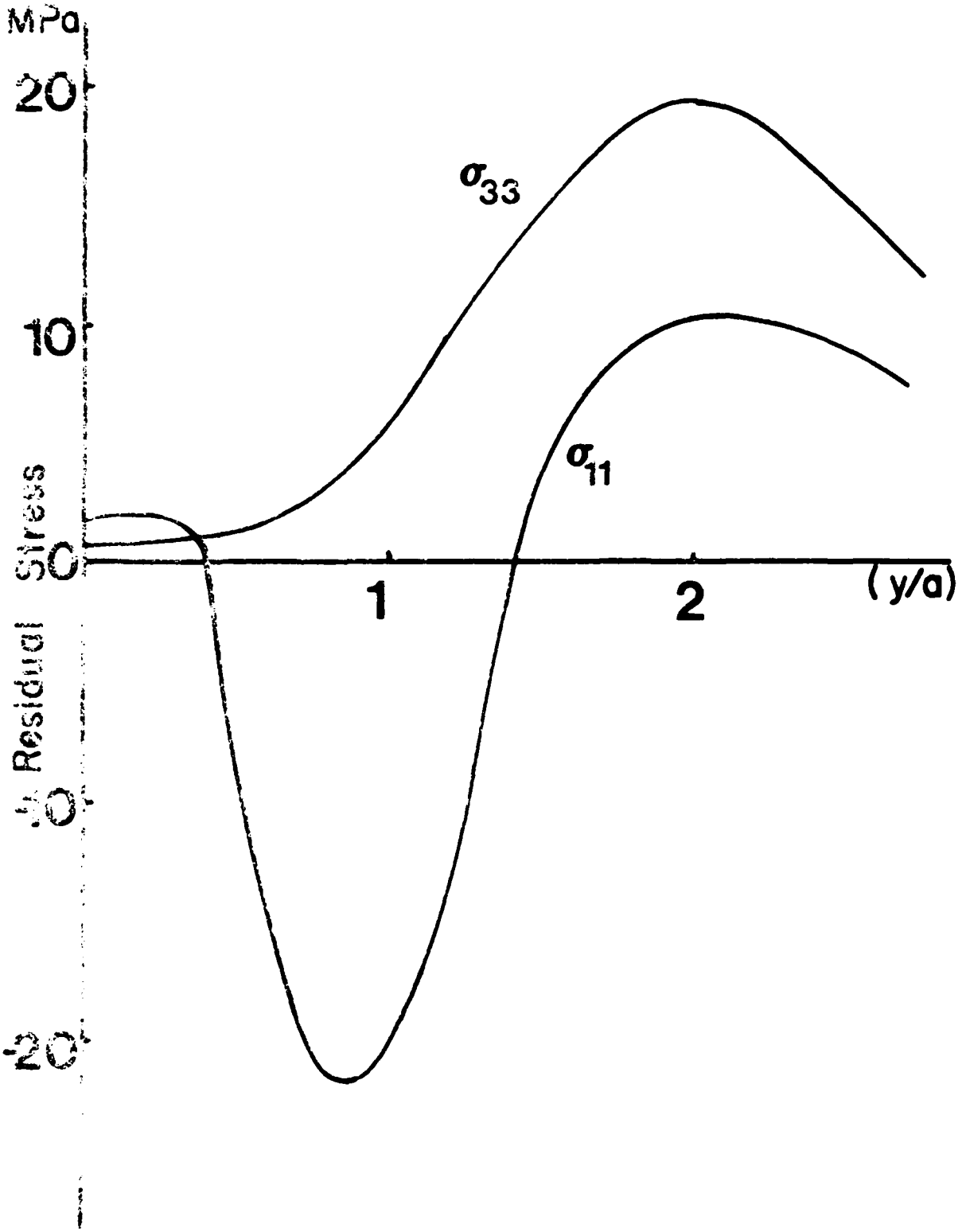

Ho, Noyan, Cohen, Khanna & Eliezer

FIGURE 1b

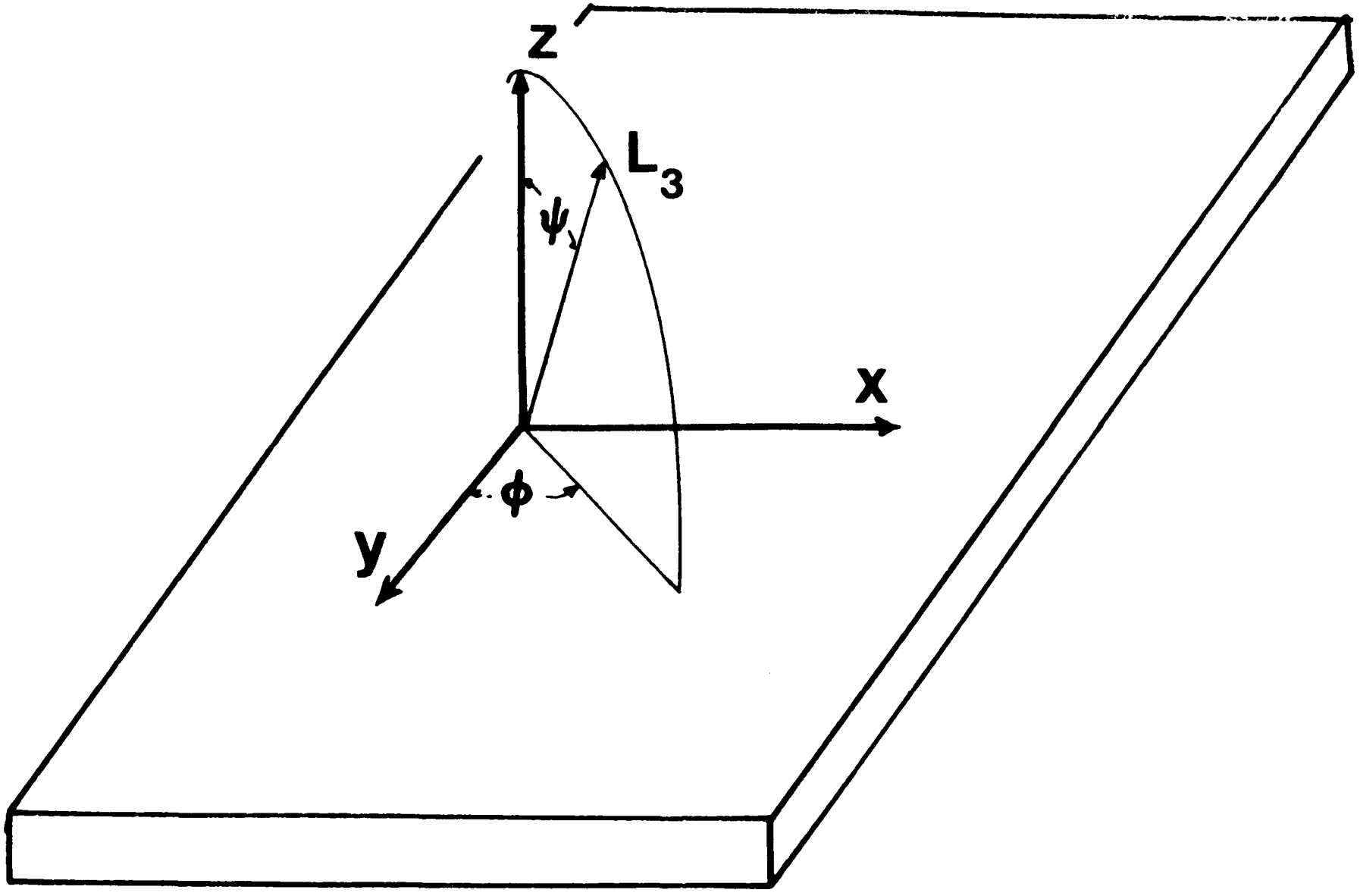

Ho, Noyan, Cohen, Khanna & Eliezer

FIGURE 2

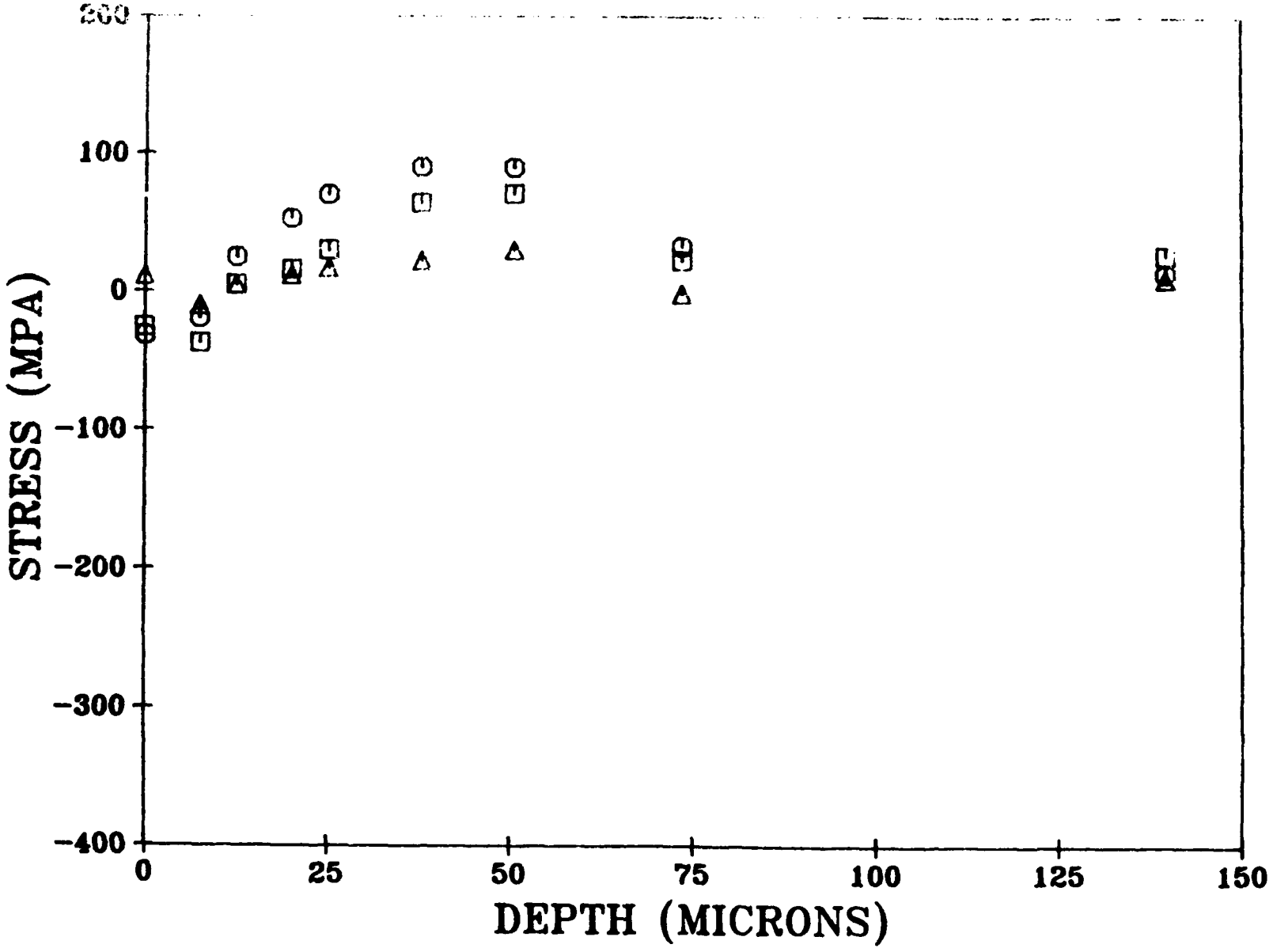

Ho, Noyan, Cohen, Khanna & Eliezer

FIGURE 3a

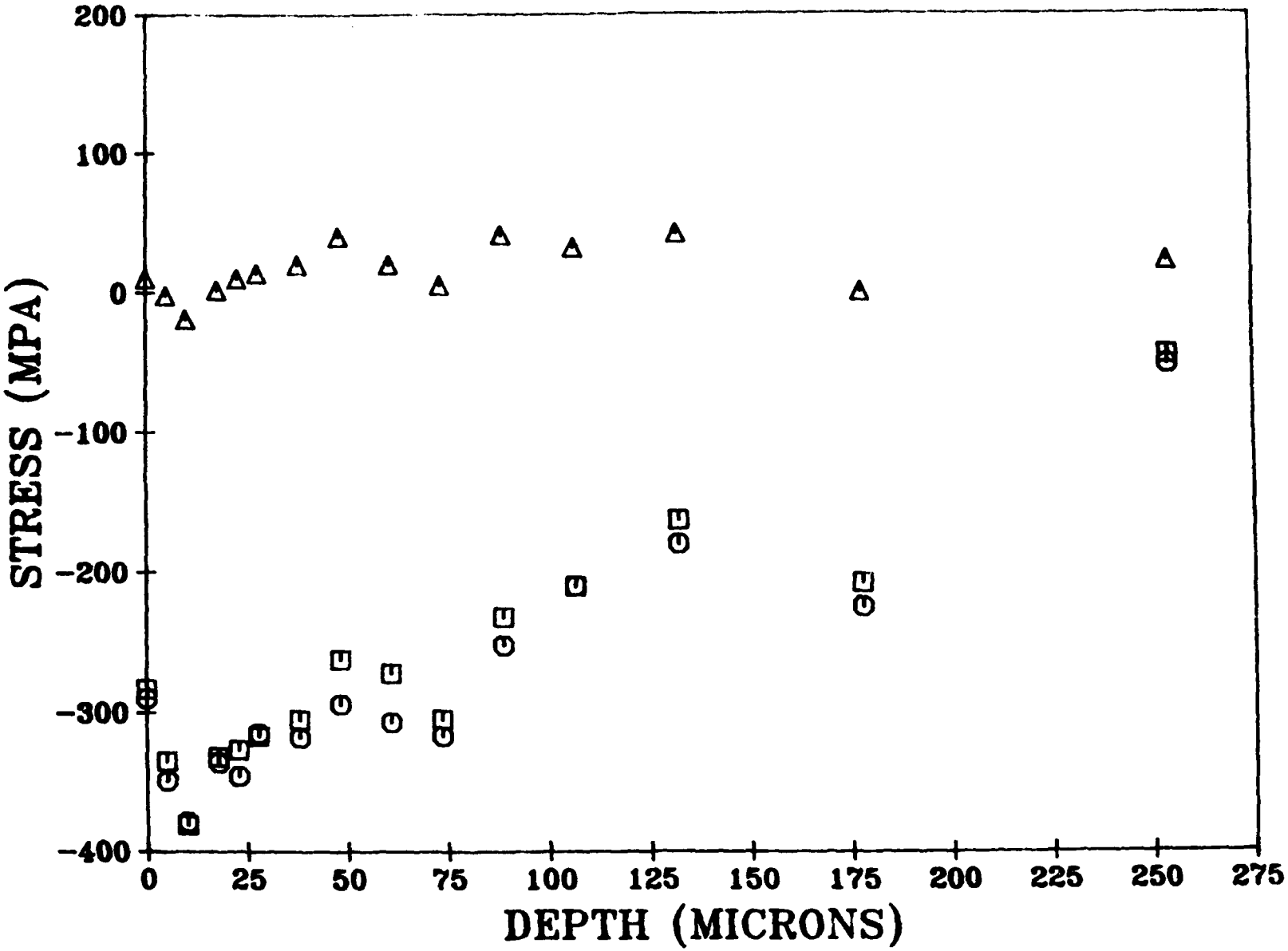

Ho, Noyan, Cohen, Khanna & Eliezer

FIGURE 3b

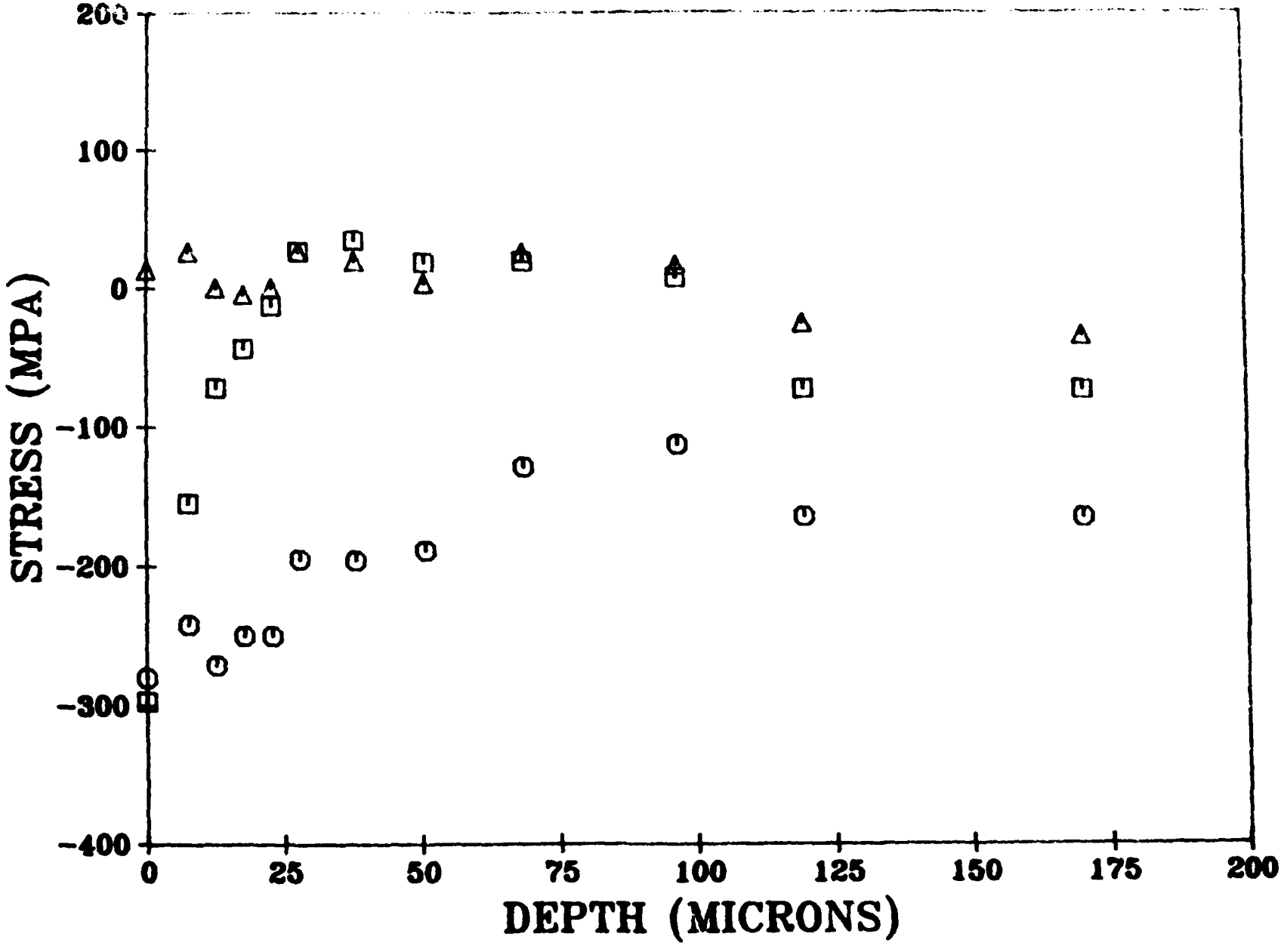

Ho, Noyan, Cohen, Khanna & Eliezer

FIGURE 3c

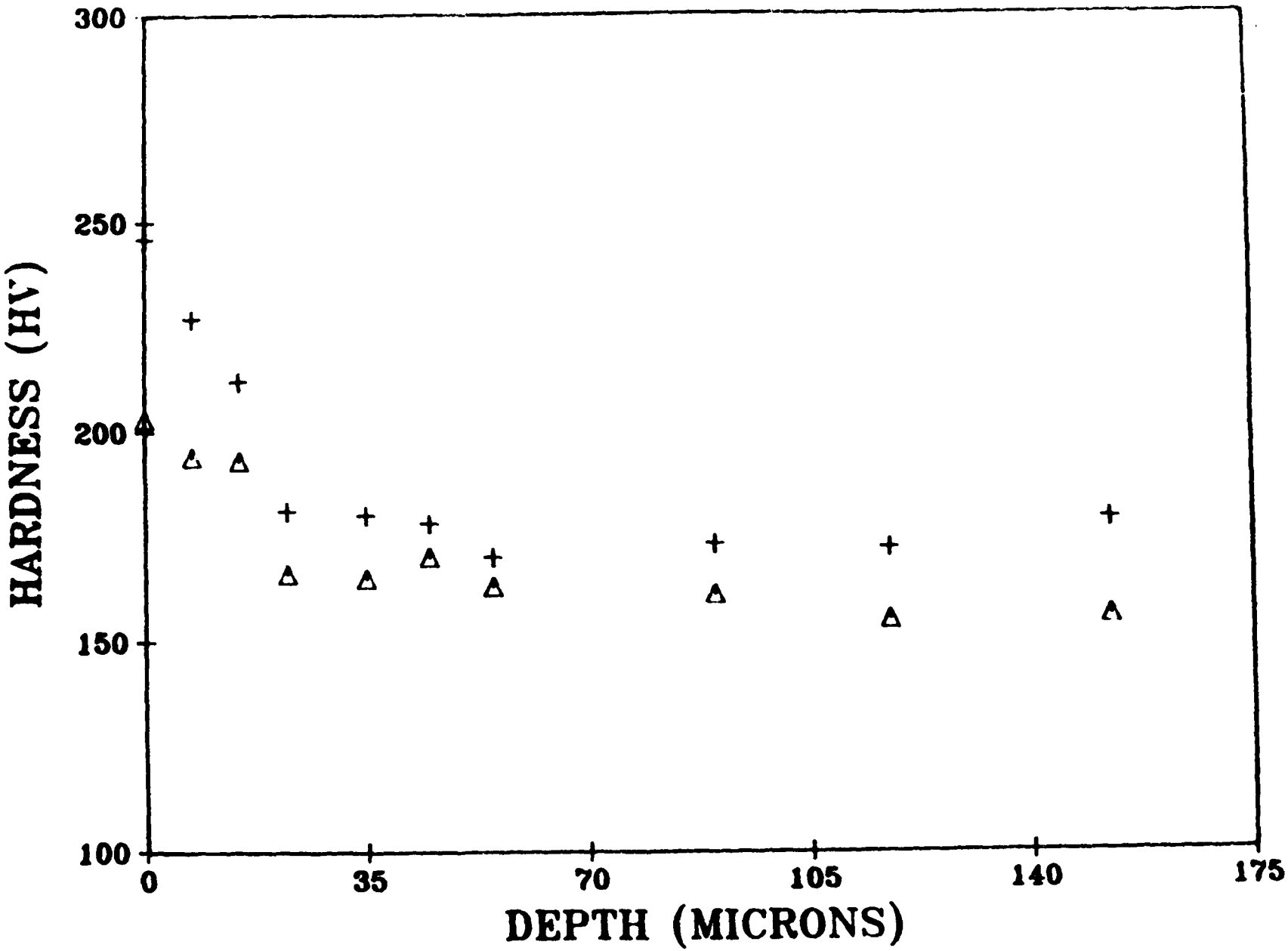

FIGURE 4a

Ho, Noyan, Cohen, Khanna & Eliezer

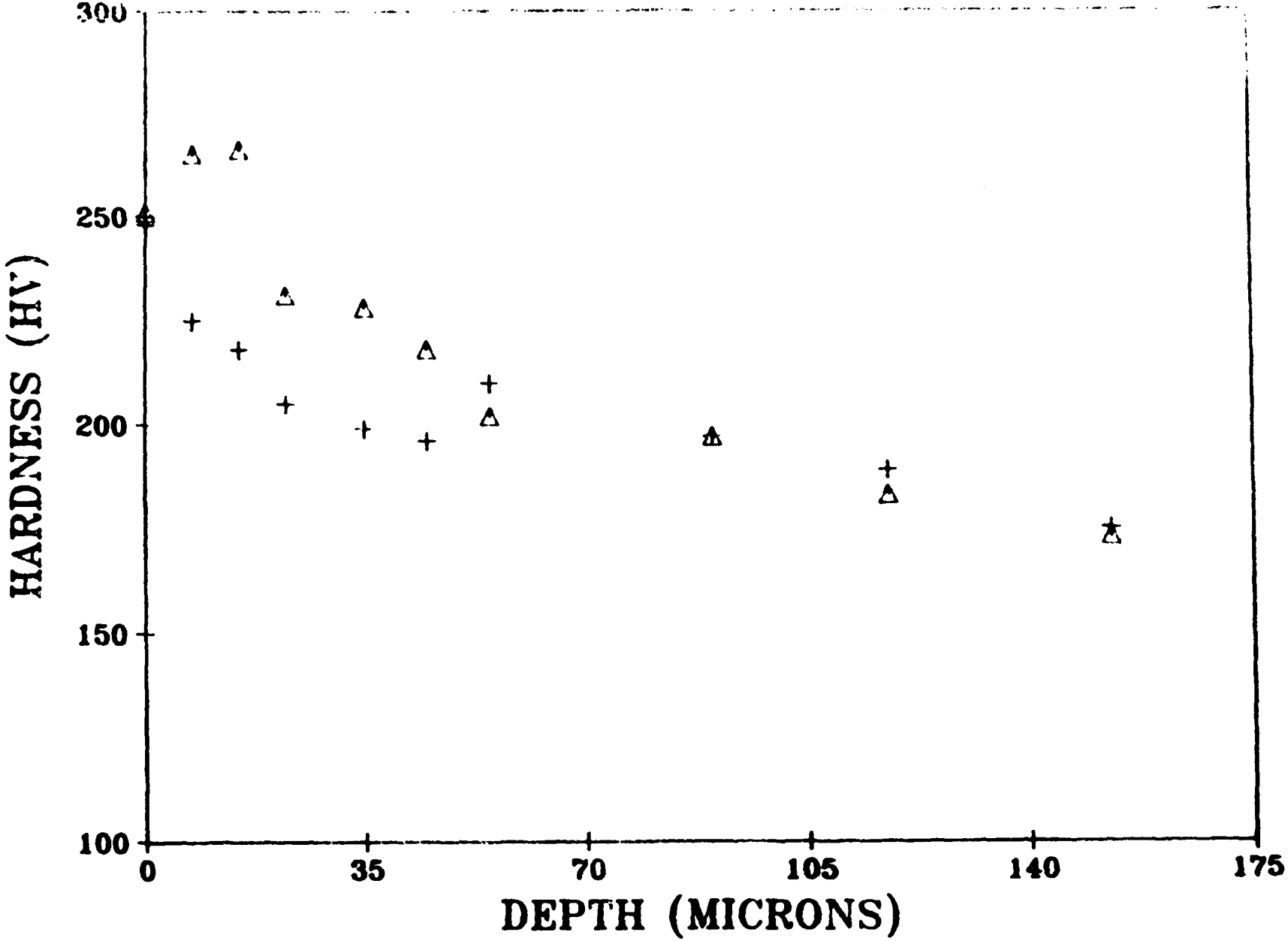

FIGURE 4b

Ho, Noyan, Cohen, Khanna & Eliezer

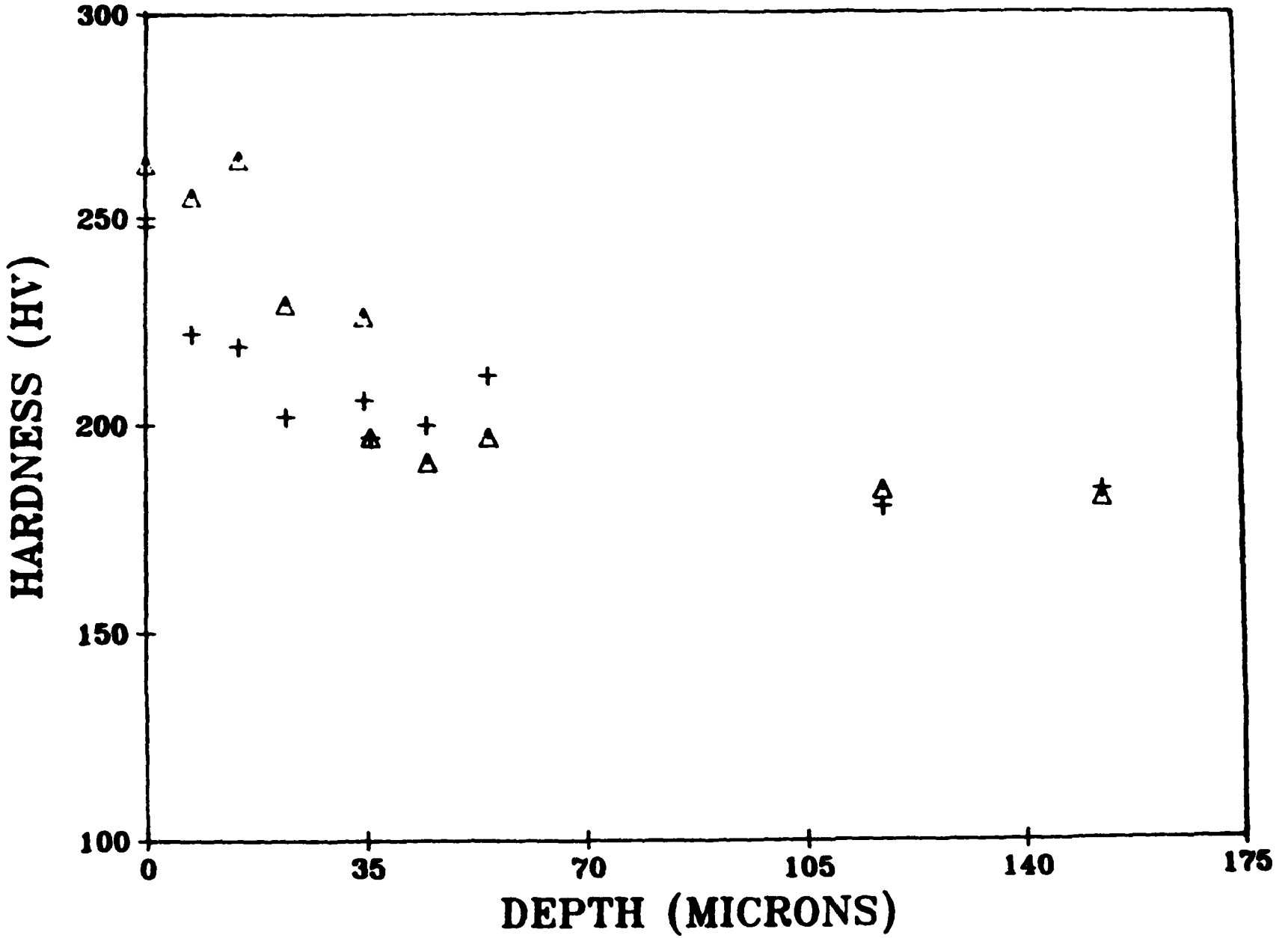

FIGURE 4c

Ho, Noyan, Cohen, Khanna and Eliezer

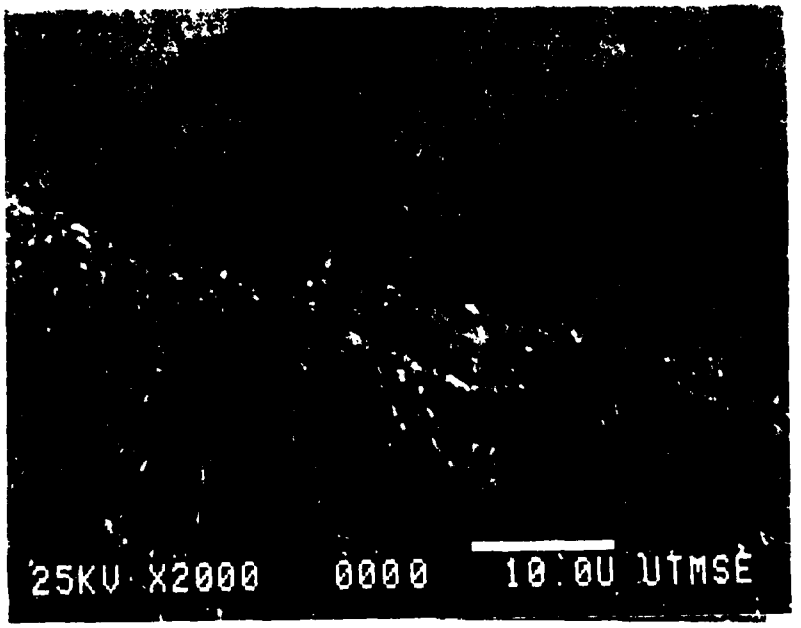

FIGURE 5

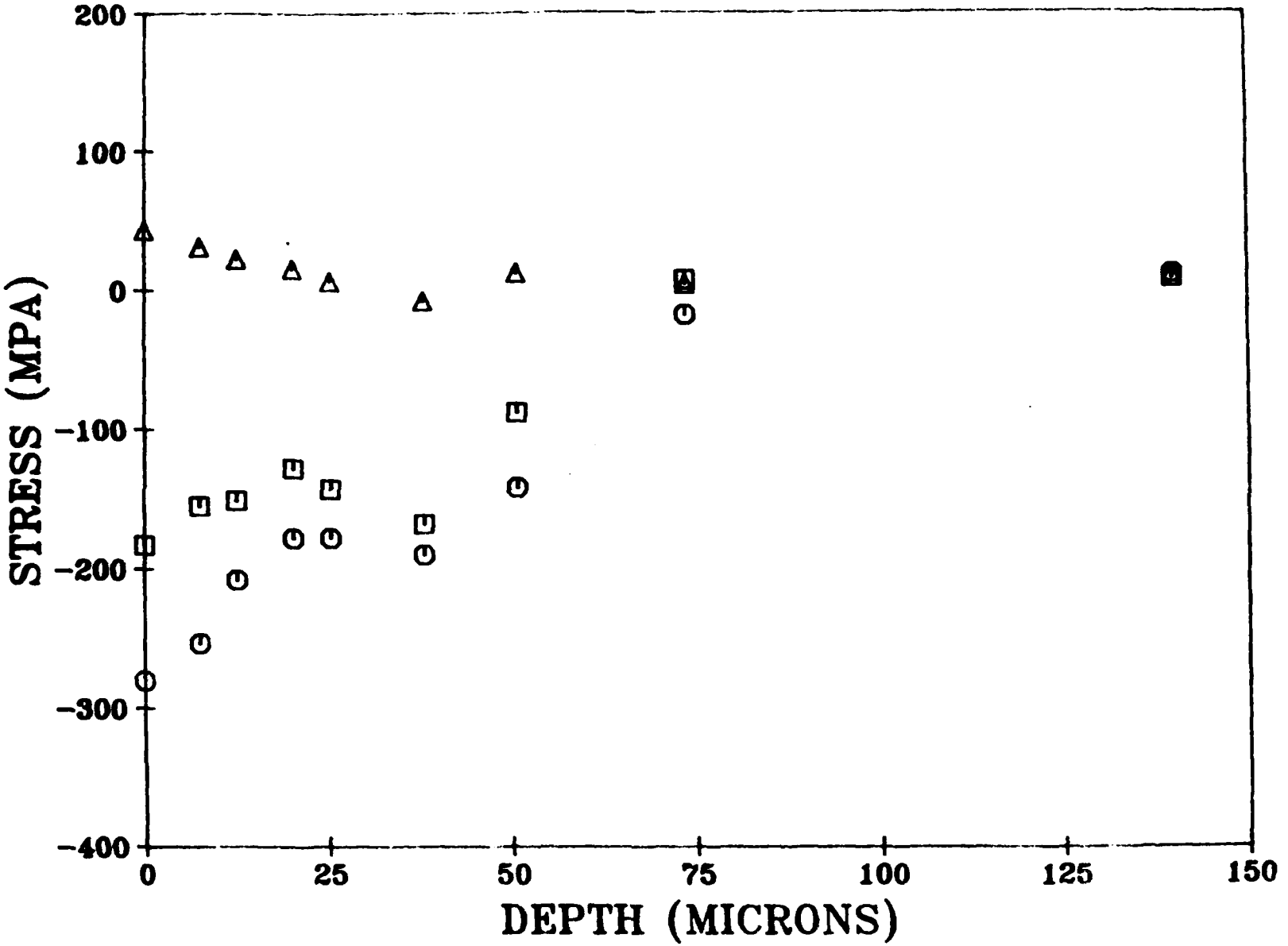

Ho, Noyan, Cohen, Khanna & Eliezer

FIGURE 6a

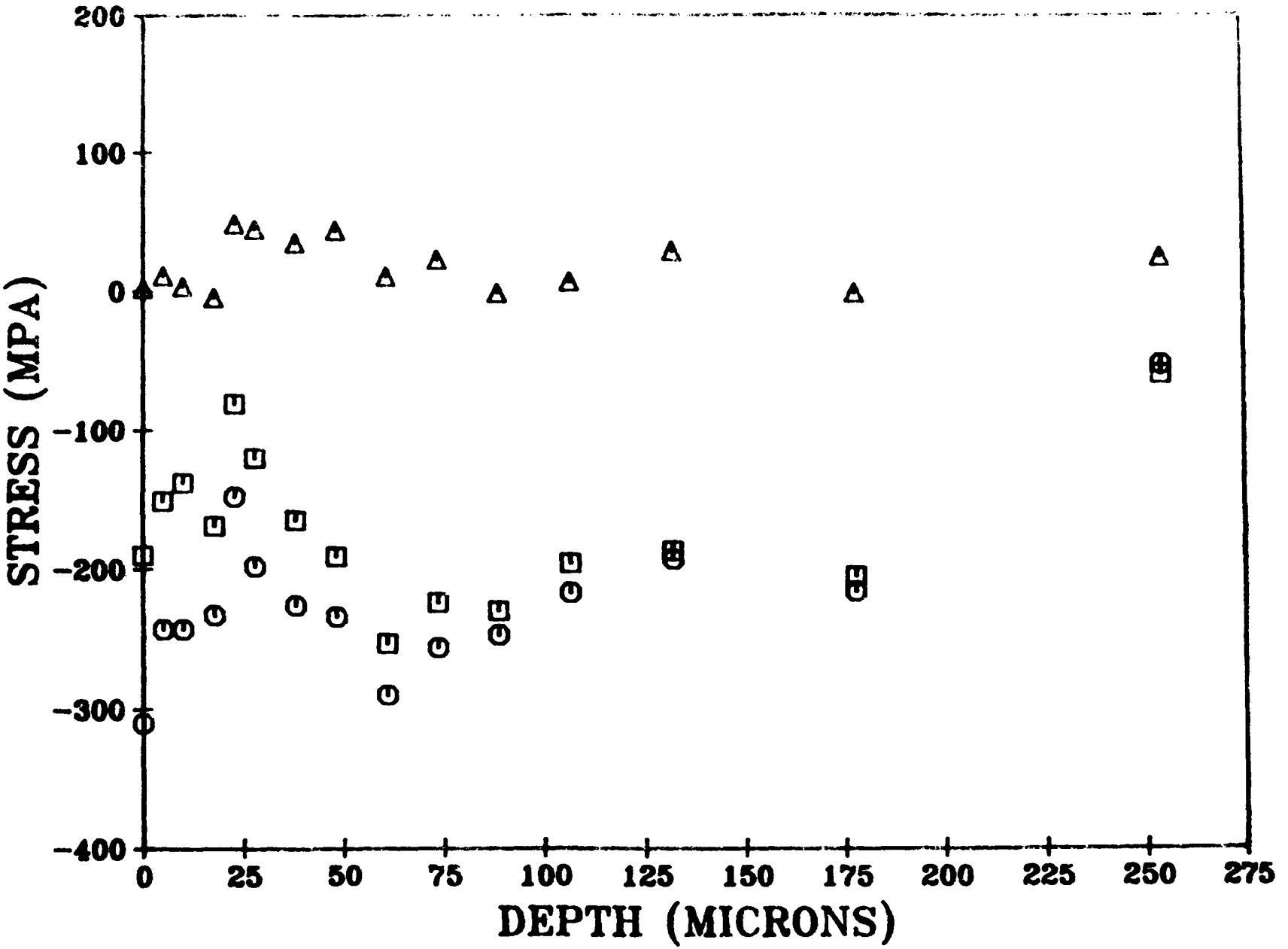

Ho, Noyan, Cohen, Khanna & Eliezer

FIGURE 6b

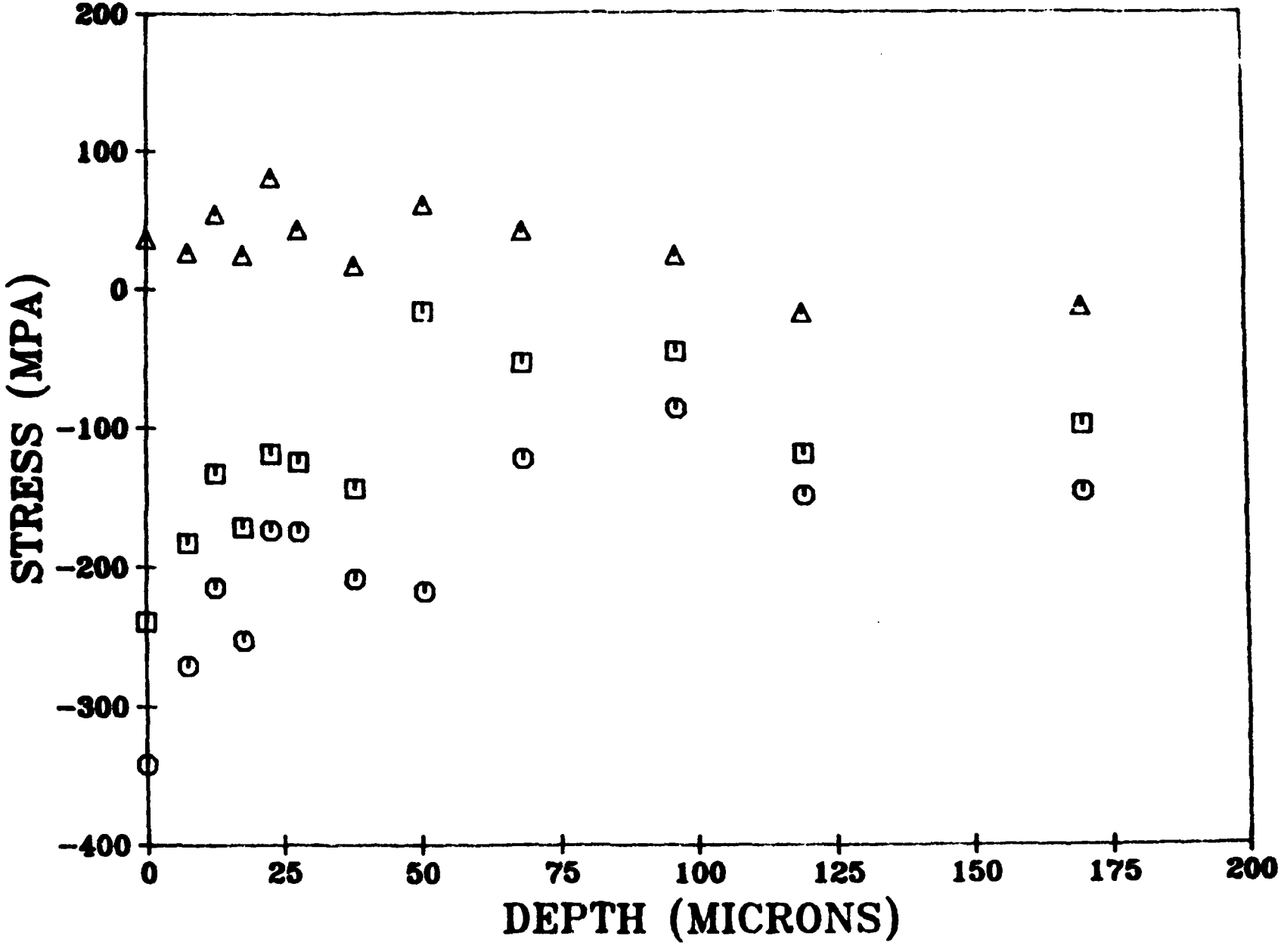

Ho, Noyan, Cohan, Khanna & Eliezer

FIGURE 6c

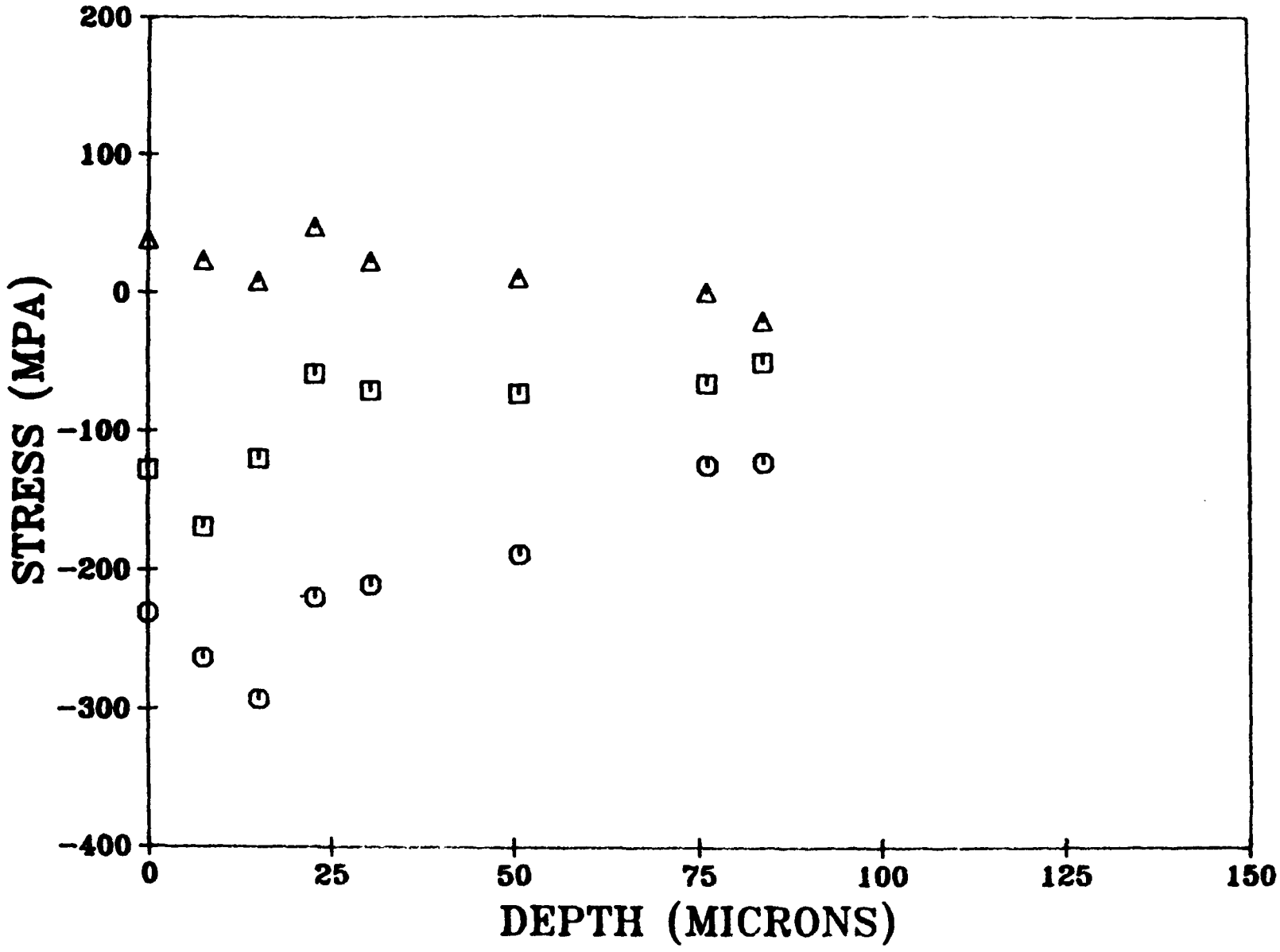

Ho, Noyan, Cohen, Khanna & Eliezer

FIGURE 7

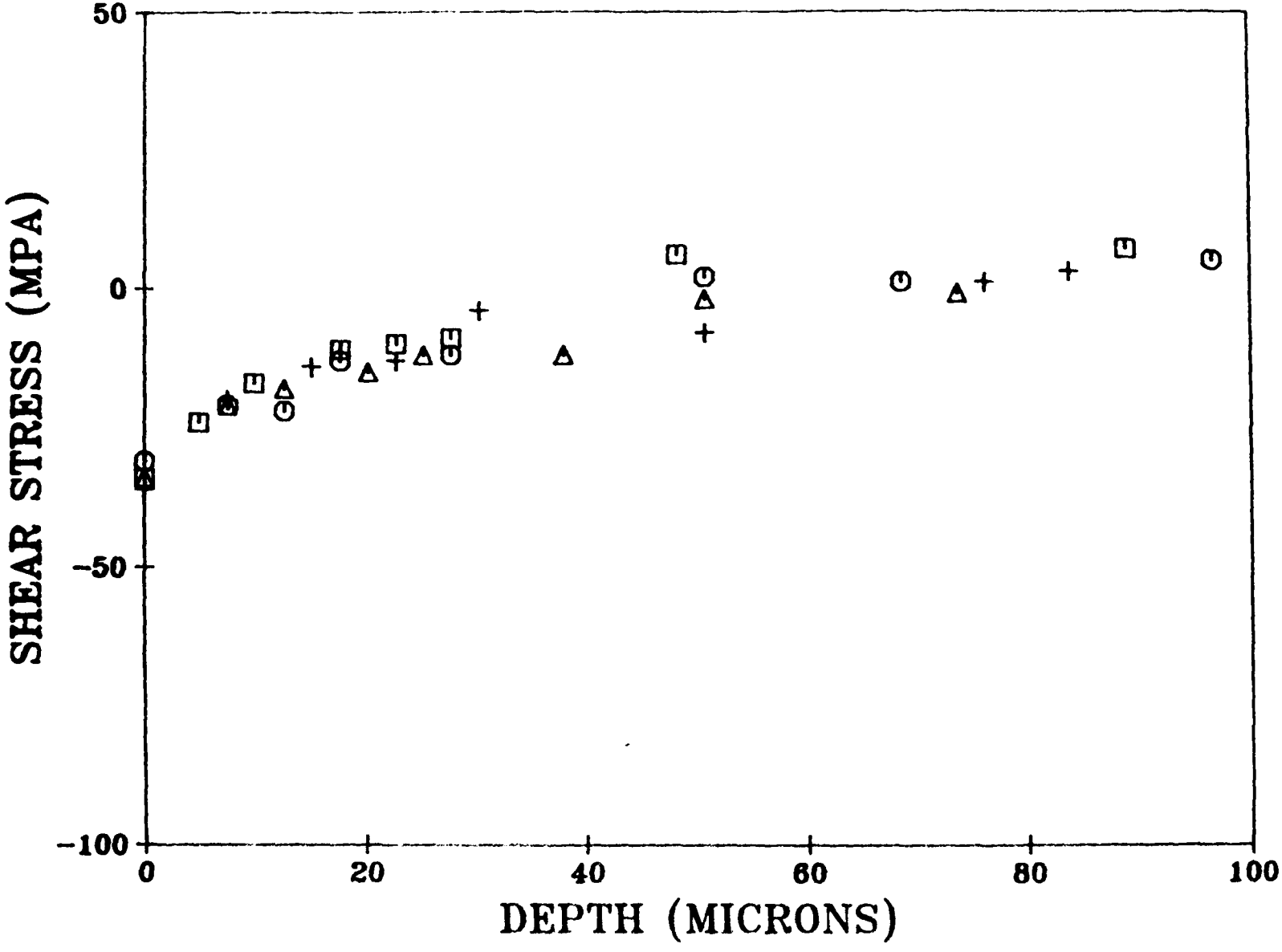

Ho, Noyan, Cohen, Khanna & Eliezer

FIGURE 8

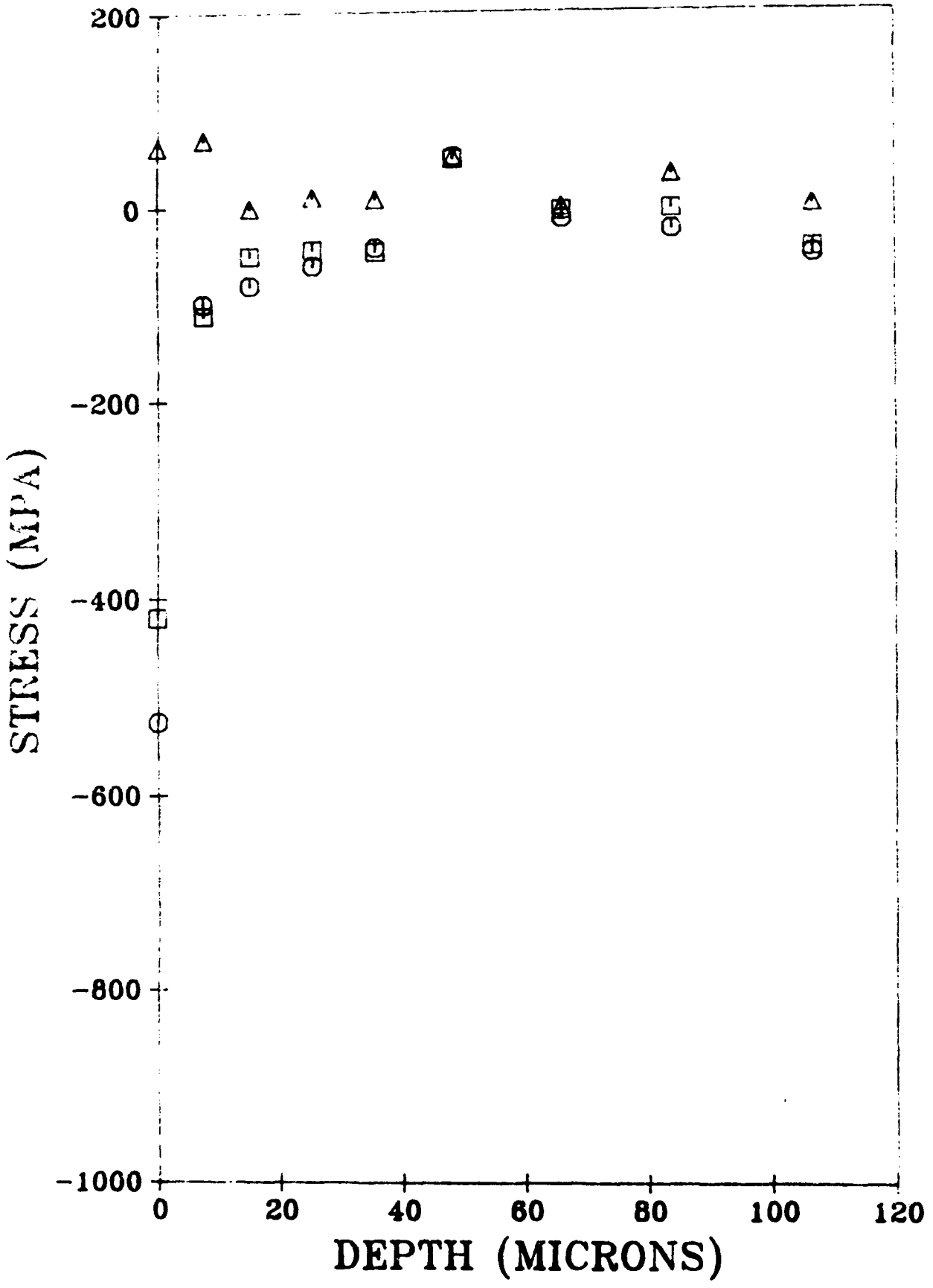

Ho, Noyan, Cohen, Khanna & Eliezer

FIGURE 9a

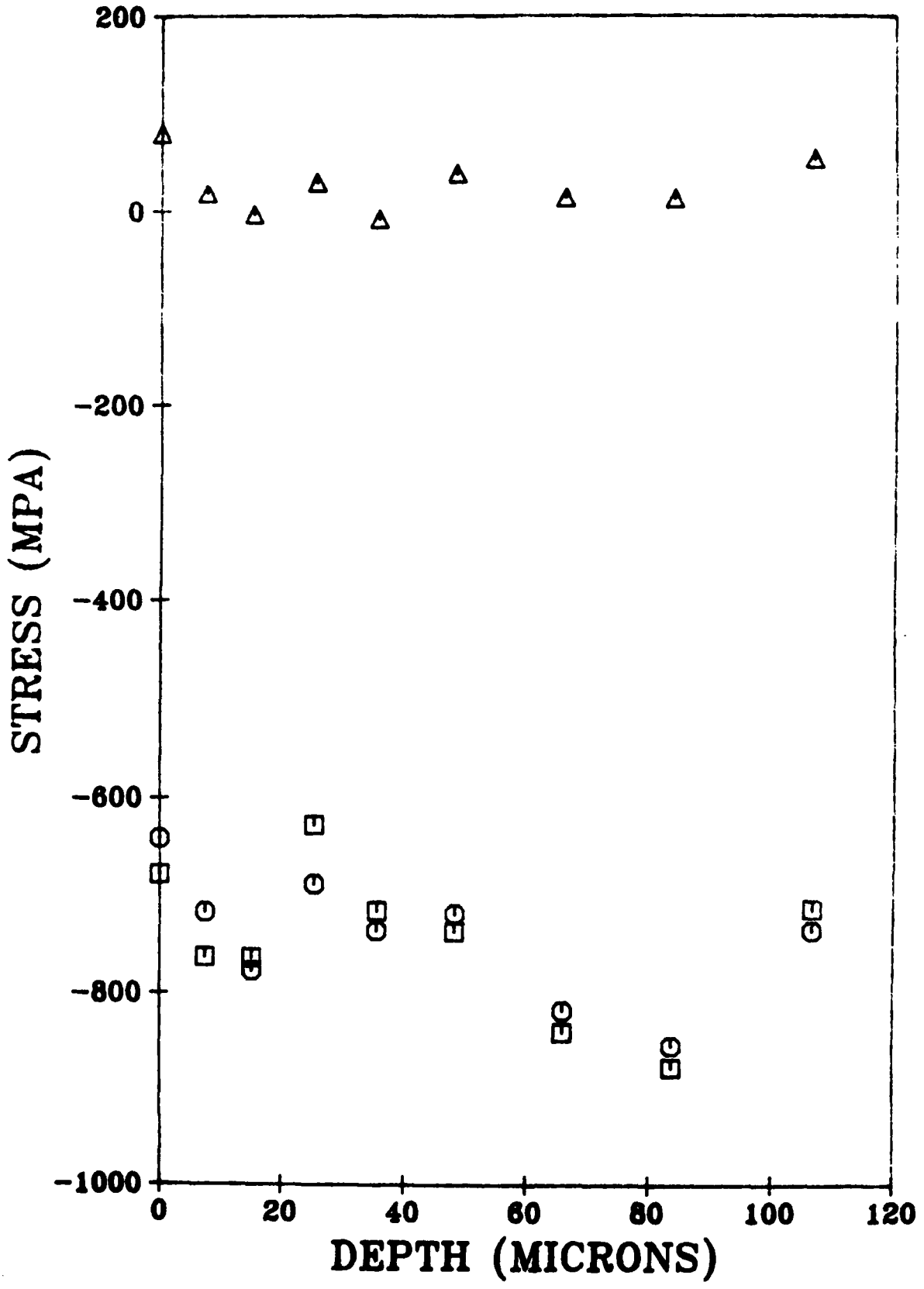

Ho, Noyan, Cohen, Khanna & Eliezer

FIGURE 9b

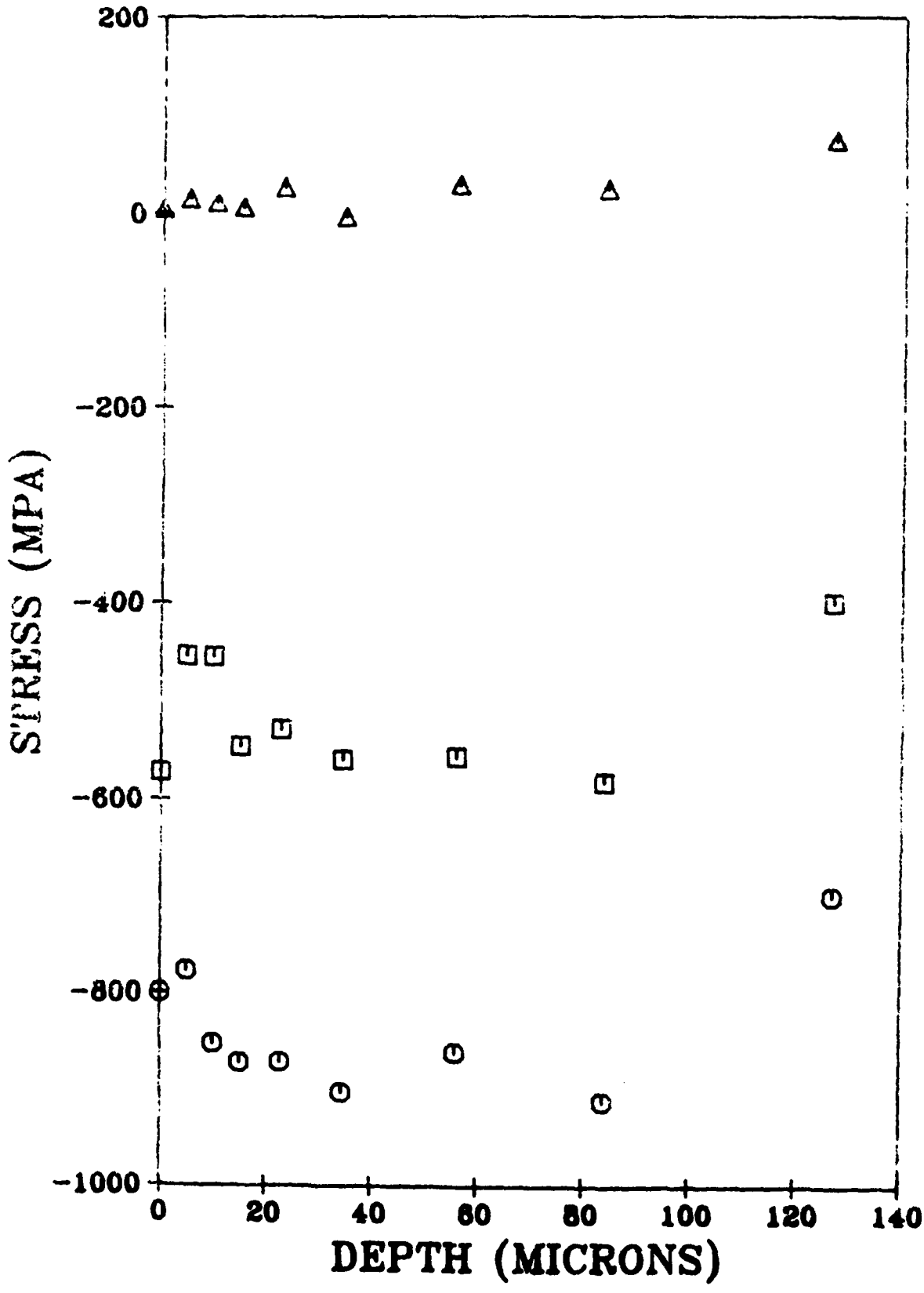

Ho, Noyan, Cohen, Khanna & Eliezer

FIGURE 9c

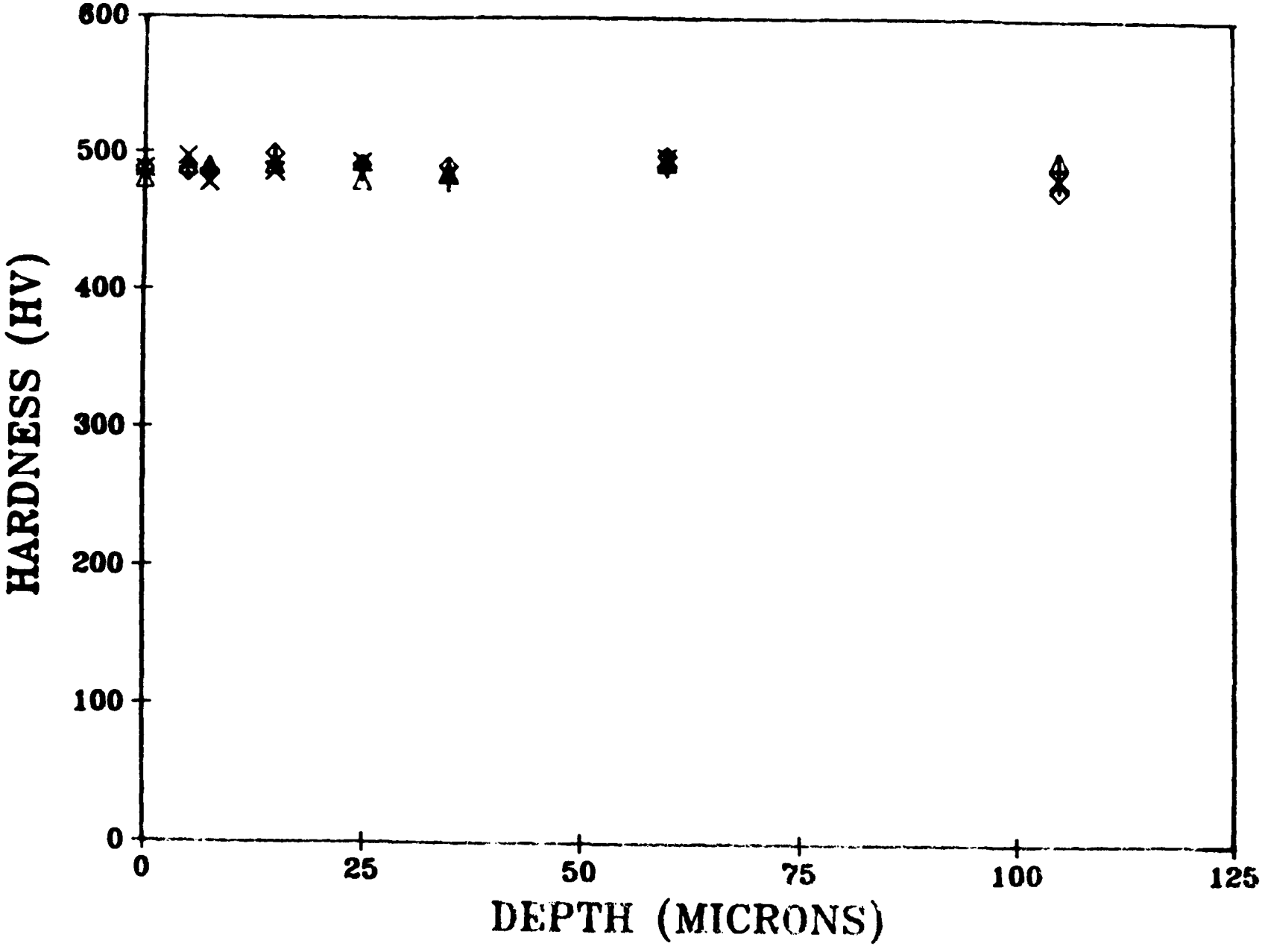

Ho, Noyan, Cohen, Khanna & Fliczer

FIGURE 10a

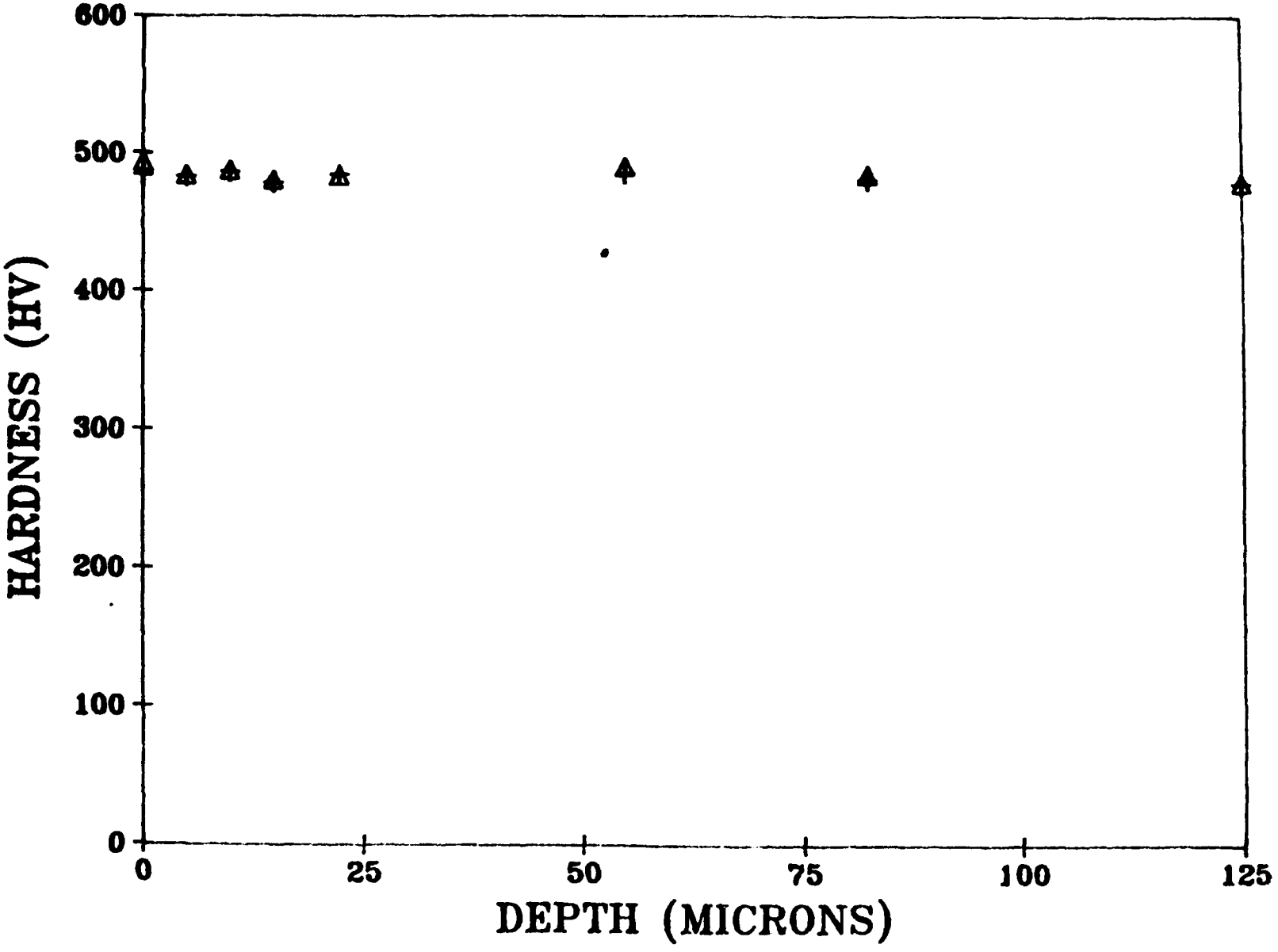

Ho, Noyan, Cohen, Khanna & Eliezer

FIGURE 10b

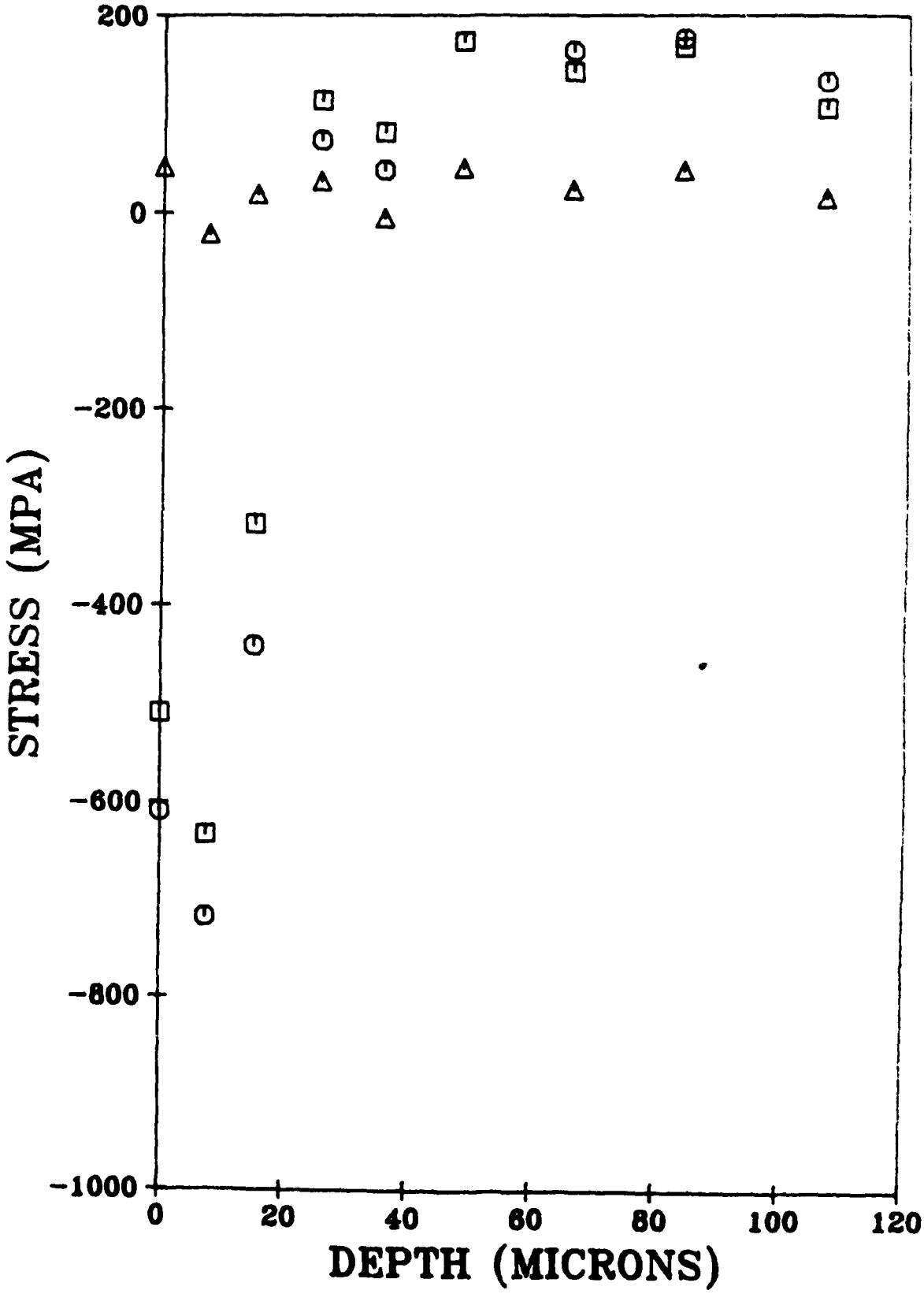

Ho, Noyan, Cohen, Khanna & Eliezer

FIGURE 11a

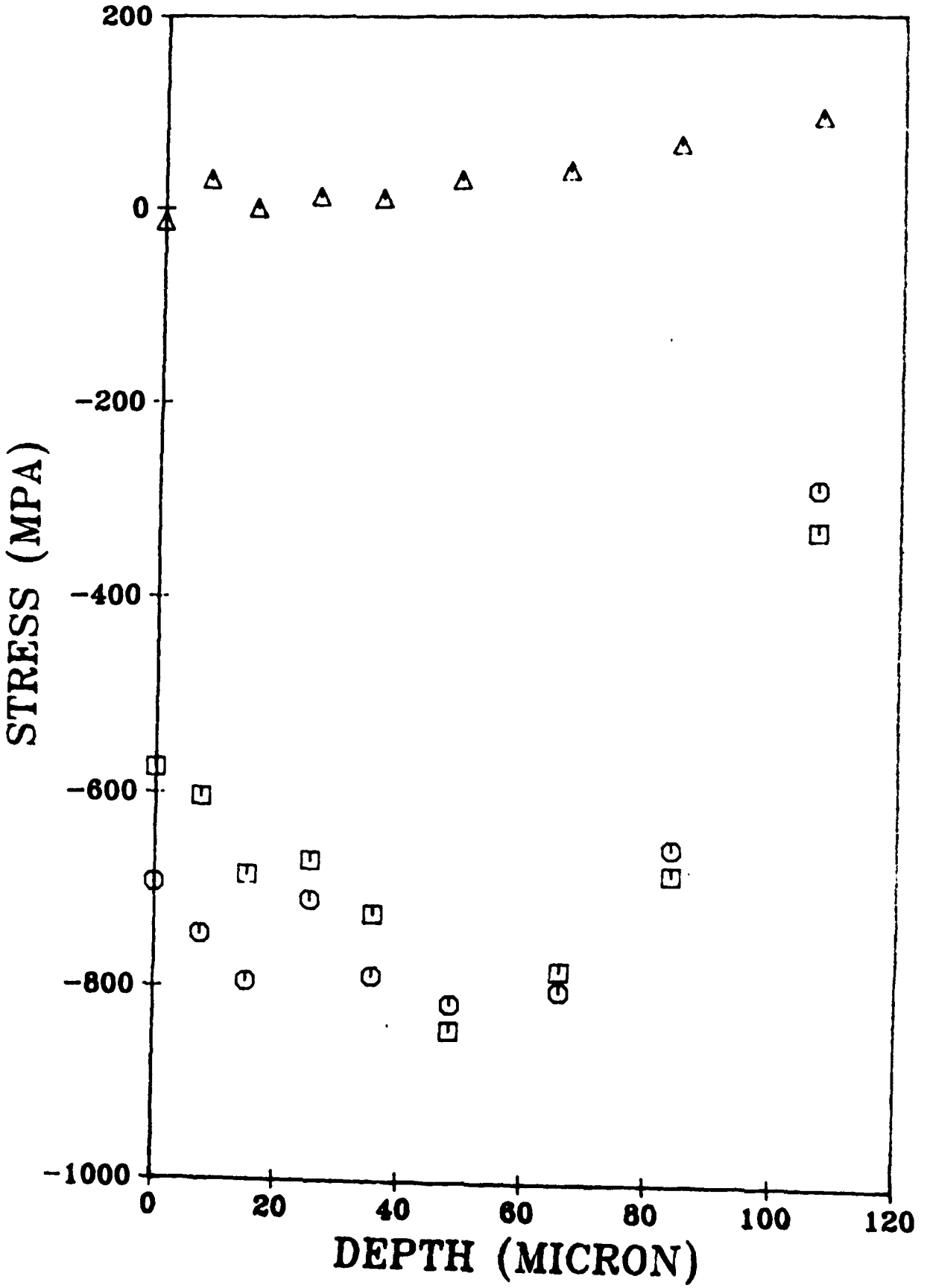

Ho, Noyan, Cohen, Khanna & Eliezer

FIGURE 11b

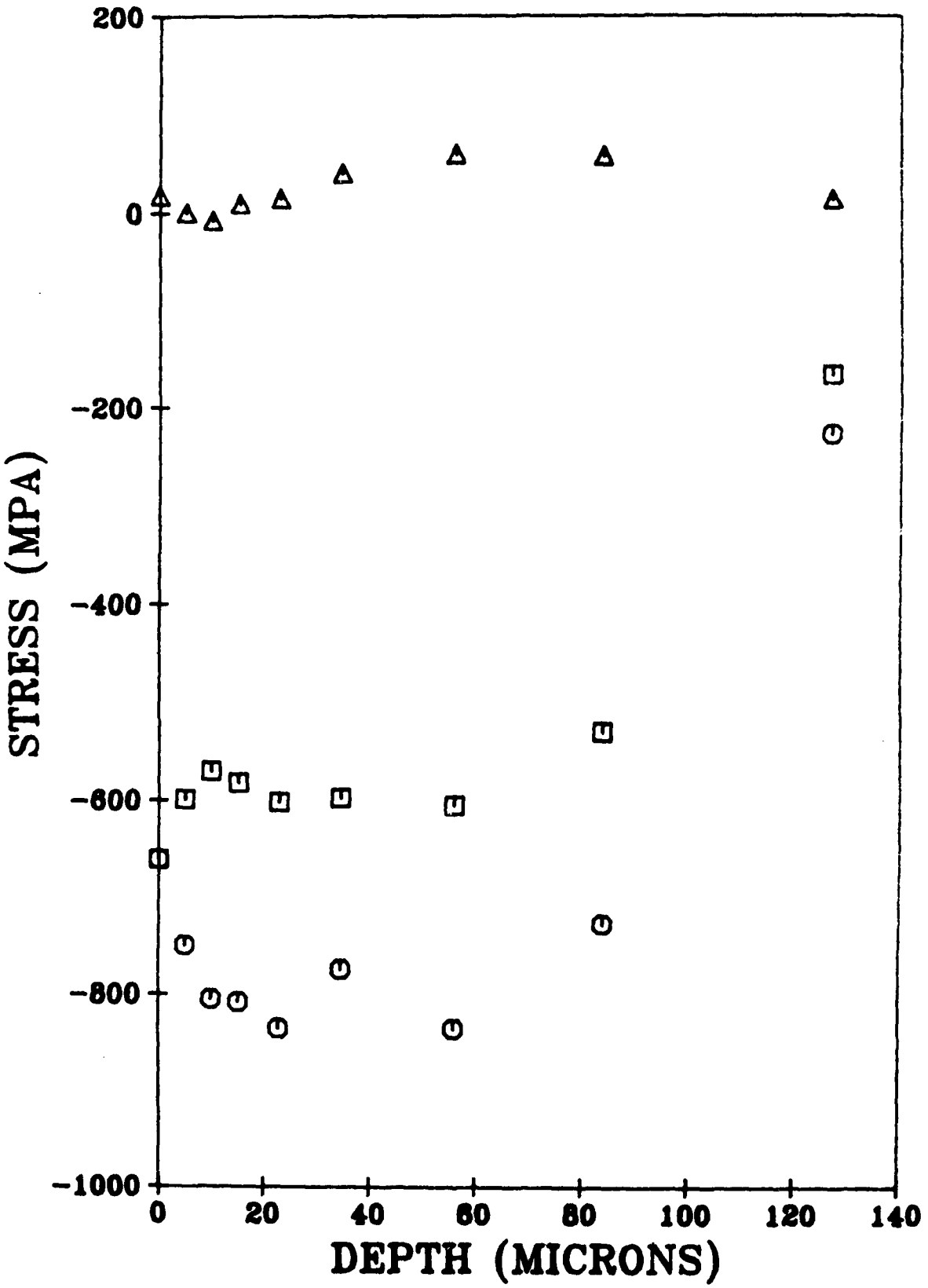

Ho, Noyan, Cohen, Khanna & Eliezer

FIGURE 11c

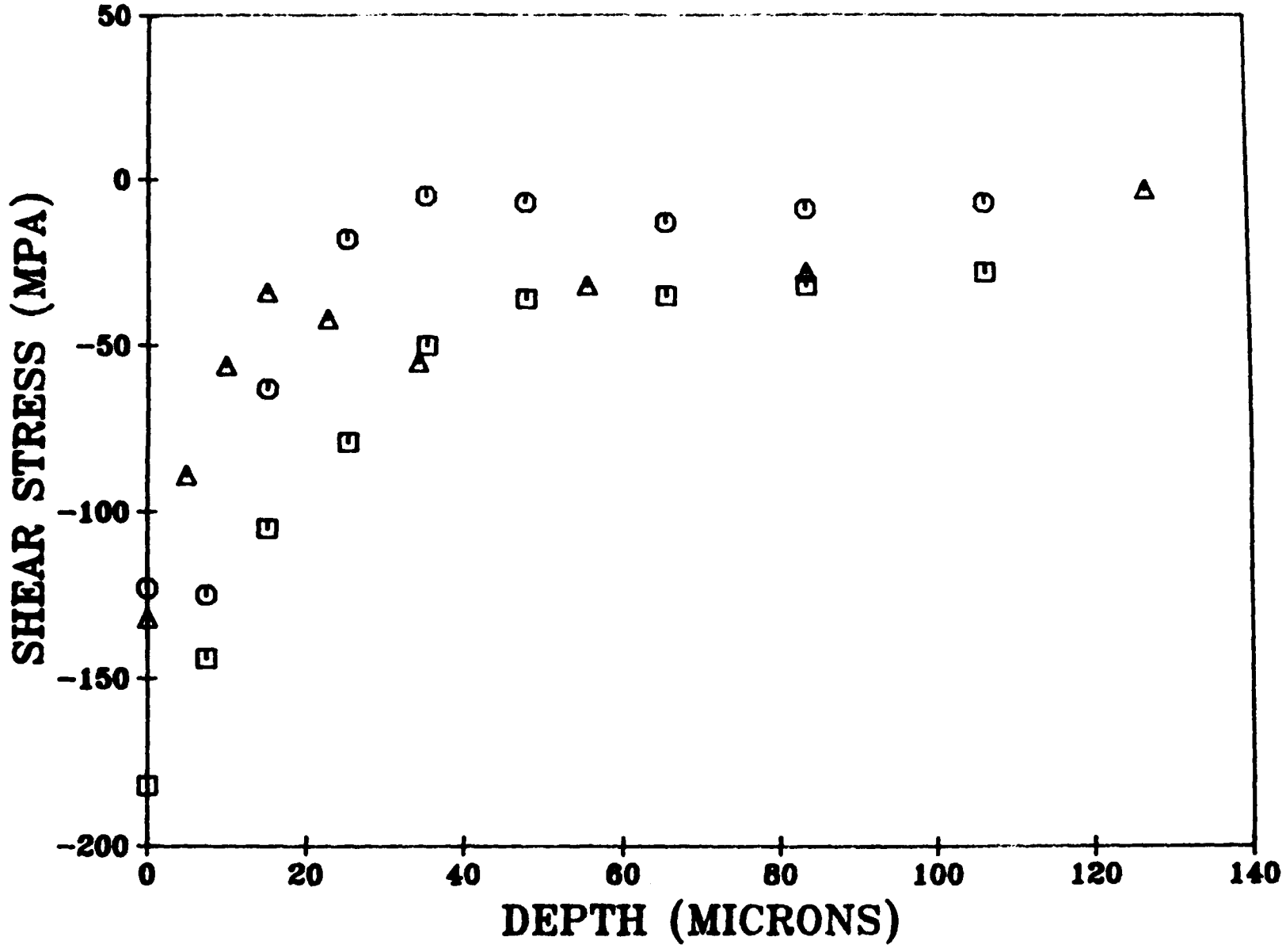

Ho, Noyan, Cohen, Khanna & Eliezer

FIGURE 12

Security Classification

DOCUMENT CONTROL DATA - R & D

(Security classification of title, body of abstract and indexing annotation must be entered when the overall report is classified)

1. ORIGINATING ACTIVITY (Corporate author)	2a. REPORT SECURITY CLASSIFICATION
J. B. Cohen Northwestern University Evanston, Illinois 60201	Unclassified 2b. GROUP

3. REPORT TITLE

RESIDUAL STRESSES AND SLIDING WEAR

4. DESCRIPTIVE NOTES (Type of report and inclusive dates)

Technical Report No. 7

5. AUTHOR(S) (First name, middle initial, last name)

J. W. Ho, C. Noyan, J. B. Cohen, V. D. Khanna and Z. Eliezer

6. REPORT DATE	7a. TOTAL NO. OF PAGES	7b. NO. OF REFS
May 25, 1982	51	21

8a. CONTRACT OR GRANT NO.	9a. ORIGINATOR'S REPORT NUMBER(S)
Nooo14-80-C-0116 b. PROJECT NO. Mod. No. P00002	7
c. d.	9b. OTHER REPORT NO(S) (Any other numbers that may be assigned this report)

10. DISTRIBUTION STATEMENT

Distribution of this document is unlimited

11. SUPPLEMENTARY NOTES	12. SPONSORING MILITARY ACTIVITY
	Metallurgy Branch Office of Naval Research

13. ABSTRACT

The residual stresses that develop during wear of SAE 1018 and 4340 steel have been examined. The entire three-dimensional stress tensor was obtained. A normal stress perpendicular to the surface, predicted by theory, has been found, but its magnitude is too small to affect the wear rate. There are also significant shear stresses. The wear process rapidly alters any initial stress distribution produced by heat treatment or peening to such a degree that the wear rate is not affected by these stresses, unless they are initially larger than those that can be produced by the wear parameters.

DD FORM 1 NOV 65 1473 (PAGE 1)

S/N 0101-807-6801

Security Classification

14. KEY WORDS	LINK A		LINK B		LINK C	
	ROLE	WT	ROLE	WT	ROLE	WT
stresses, residual stresses, wear						

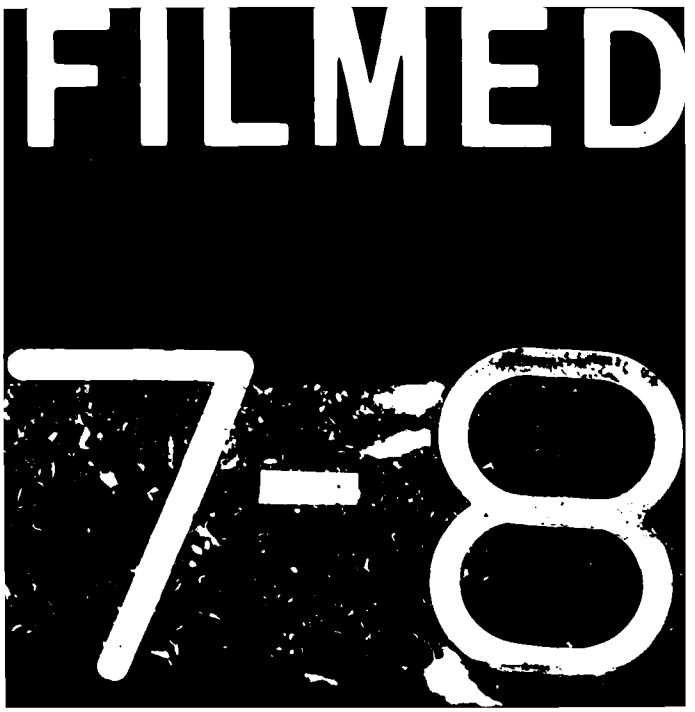
FILMED
7-8